

Neurofibromatosis from Head to Toe: What the Radiologist Needs to Know

Mindy X. Wang, MD
 Jonathan R. Dillman, MD, MSc
 Jeffrey Guccione, MD
 Ahmed Habiba, MD
 Marwa Maher, MD
 Serageldin Kamel, MD
 Prasad M. Panse, MD
 Corey T. Jensen, MD
 Khaled M. Elsayes, MD

Abbreviations: CNS = central nervous system, FASI = focal area of signal intensity, NF1 = neurofibromatosis type 1, NF2 = neurofibromatosis type 2, PNST = peripheral nerve sheath tumor

RadioGraphics 2022; 42:1123–1144

<https://doi.org/10.1148/rg.210235>

Content Codes: **CT** **GI** **GU** **MR** **NR** **PD**

From the Department of Radiology (M.X.W., C.T.J., K.M.E.) and Department of Lymphoma and Myeloma (S.K.), University of Texas MD Anderson Cancer Center, Pickens Academic Tower, 1400 Pressler St, Houston, TX 77030-4009; Department of Radiology, Cincinnati Children's Hospital Medical Center, University of Cincinnati, Cincinnati, Ohio (J.R.D.); Department of Radiology, Stanford University, Stanford, Calif (J.G.); Department of Radiology (A.H.) and Faculty of Medicine (M.M.), Alexandria University, Alexandria, Egypt; and Department of Radiology, Mayo Clinic Arizona, Phoenix/Scottsdale, Ariz (P.M.P.). Presented as an education exhibit at the 2021 RSNA Annual Meeting. Received December 30, 2021; revision requested January 26, 2022, and received February 17; accepted February 18. For this journal-based SA-CME activity, the author K.M.E. has provided disclosures (see end of article); all other authors, the editor, and the reviewers have disclosed no relevant relationships. **Address correspondence** to M.X.W. (email: Mindy.X.Wang@uth.tmc.edu).

©RSNA, 2022

SA-CME LEARNING OBJECTIVES

After completing this journal-based SA-CME activity, participants will be able to:

- Describe the diagnostic criteria for NF1 and NF2.
- Identify characteristic NF1-related imaging manifestations.
- Recognize characteristic NF2-related imaging manifestations.

See rsna.org/learning-center-rg.

Neurofibromatosis type 1 (NF1) and neurofibromatosis type 2 (NF2) are autosomal dominant inherited neurocutaneous disorders or phakomatoses secondary to mutations in the *NF1* and *NF2* tumor suppressor genes, respectively. Although they share a common name, NF1 and NF2 are distinct disorders with a wide range of multisystem manifestations that include benign and malignant tumors. Imaging plays an essential role in diagnosis, surveillance, and management of individuals with NF1 and NF2. Therefore, it is crucial for radiologists to be familiar with the imaging features of NF1 and NF2 to allow prompt diagnosis and appropriate management. Key manifestations of NF1 include café-au-lait macules, axillary or inguinal freckling, neurofibromas or plexiform neurofibromas, optic pathway gliomas, Lisch nodules, and osseous lesions such as sphenoid dysplasia, all of which are considered diagnostic features of NF1. Other manifestations include focal areas of signal intensity in the brain, low-grade gliomas, interstitial lung disease, various abdominopelvic neoplasms, scoliosis, and vascular dysplasia. The various NF1-associated abdominopelvic neoplasms can be categorized by their cellular origin: neurogenic neoplasms, interstitial cells of Cajal neoplasms, neuroendocrine neoplasms, and embryonal neoplasms. Malignant peripheral nerve sheath tumors and intracranial tumors are the leading contributors to mortality in NF1. Classic manifestations of NF2 include schwannomas, meningiomas, and ependymomas. However, NF2 may have shared cutaneous manifestations with NF1. Lifelong multidisciplinary management is critical for patients with either disease. The authors highlight the genetics and molecular pathogenesis, clinical and pathologic features, imaging manifestations, and multidisciplinary management and surveillance of NF1 and NF2.

Online supplemental material is available for this article.

©RSNA, 2022 • radiographics.rsna.org

Introduction

Neurofibromatosis type 1 (NF1) and neurofibromatosis type 2 (NF2) are autosomal dominant inherited neurocutaneous disorders or phakomatoses that share a common name; however, they are distinct disorders with a wide range of clinical and imaging manifestations. NF1, also known as von Recklinghausen disease, is the most common phakomatosis. Key clinical manifestations of NF1 include café-au-lait macules, axillary or inguinal freckling, neurofibromas or plexiform neurofibromas, optic pathway gliomas, Lisch nodules, and osseous lesions such as sphenoid dysplasia, which are considered diagnostic features. However, there are numerous other manifestations, such as low-grade gliomas, interstitial lung disease, various abdominopelvic neoplasms, scoliosis, and vascular dysplasia.

Classic manifestations of NF2 include schwannomas, meningiomas, and ependymomas. This article highlights the genetics and molecular

TEACHING POINTS

- At MRI, FASIs demonstrate focal or diffuse hyperintensity in the basal ganglia, cerebellum, or brainstem at T2-weighted imaging and fluid-attenuated inversion-recovery (FLAIR) imaging, relative to the brain. They generally exhibit isointensity or mild hyperintensity at T1-weighted imaging, no enhancement, and no mass effect. At MR spectroscopy, they demonstrate preserved *N*-acetylaspartate level, unlike gliomas.
- Gliomas are distinguished from FASIs by the presence of mass effect, their T1 and T2 characteristics, contrast enhancement, and evolution over time. MR spectroscopy can also help differentiate these from FASIs, as gliomas demonstrate decreased or absent *N*-acetylaspartate, increased choline, and decreased creatine levels.
- At MRI, malignant degeneration is suggested by heterogeneous signal intensity on T1-weighted images. Four imaging features can help differentiate malignant PNST from benign neurofibroma at MRI: large dimension of the mass, peripheral enhancement pattern, perilesion edema-like zone, and intratumor cystic changes.
- The various NF1-associated intra-abdominal neoplasms can be categorized by their cellular origin: neurogenic neoplasms, interstitial cells of Cajal neoplasms, neuroendocrine neoplasms, and embryonal neoplasms.
- Key NF2 manifestations include schwannomas, meningiomas, and ependymomas.

pathogenesis, clinical and pathologic features, imaging manifestations, and multidisciplinary management and surveillance of NF1 and NF2.

Genetics and Molecular Pathogenesis

Neurofibromatosis Type 1

NF1 has a prevalence of at least one in 4000–5000 (1). It is an autosomal dominant syndrome, resulting from loss-of-function mutations in the tumor suppressor gene *NF1*, located at chromosome 17q11.2 (2). Approximately 50% of *NF1* mutations are sporadic (2). The *NF1* gene encodes for the neurofibromin protein, a guanosine triphosphatase (GTPase)-activating protein, which normally allows inactivation of RAS proteins and inhibits proliferative growth. This syndrome follows the Knudson two-hit hypothesis, with subsequent somatic mutations causing loss of heterozygosity (2).

With *NF1* mutations, the RAS pathway is hyperactivated, leading to increased signaling through the Raf/MEK/ERK mitogen-activated protein kinase (MAPK) and phosphoinositide-3-kinase (PI3K)/AKT/mammalian target of rapamycin (mTOR) pathways. This permits increased cell proliferation, migration, and survival, resulting in various benign and malignant tumor manifestations (3).

Neurofibromatosis Type 2

NF2 has a prevalence of one in 60 000 (1). NF2 also exhibits autosomal dominant inheritance and results from loss-of-function mutations in the

Table 1: Revised Diagnostic Criteria for NF1

A: The diagnostic criteria for NF1 are met in an individual who does not have a parent diagnosed with NF1 if two or more of the following are present:

- Six or more café-au-lait macules over 5 mm in greatest diameter in prepubertal individuals and over 15 mm in greatest diameter in postpubertal individuals
- Freckling in the axillary or inguinal region
- Two or more neurofibromas of any type or one plexiform neurofibroma
- Optic pathway glioma
- Two or more iris Lisch nodules identified by slit lamp examination or two or more choroidal abnormalities
- A distinctive osseous lesion such as sphenoid dysplasia, anterolateral bowing of the tibia, or pseudarthrosis of a long bone
- A heterozygous pathogenic *NF1* variant with a variant allele fraction of 50% in apparently normal tissue such as white blood cells

B: A child of a parent who meets the diagnostic criteria specified in A merits a diagnosis of NF1 if one or more of the criteria in A are present

Source.—Reprinted, under a CC BY 4.0 license, from reference 7.

NF2 gene located at chromosome 22q11.2. The *NF2* gene encodes for the merlin protein, which regulates cell growth, especially in Schwann cells, and cell-cell adhesion (1,3). Merlin deficiency results in elevated receptor tyrosine kinase level, which activates the ERK and AKT/mTOR pathways, resulting in cell growth (3).

More than 50% of individuals present with de novo gene mutations. Approximately 20%–30% of individuals with NF2 without a family history display mosaicism, resulting in mild generalized or unilateral disease (1). Truncating mutations cause the most severe disease, while single or multiple exon deletions cause milder disease (4).

Diagnostic Criteria

Neurofibromatosis Type 1

Clinical manifestations can vary significantly among NF1 patients. While some clinical features may appear in infancy or early childhood, most hallmark features may manifest only later in life (5). Since the National Institutes of Health (NIH) Consensus Conference in 1987 (6), significant progress has been made in understanding the molecular basis of NF1. In 2020, an international panel of experts updated the diagnostic criteria for NF1, which incorporated new clinical features and genetic testing (Table 1) (Fig 1) (7).

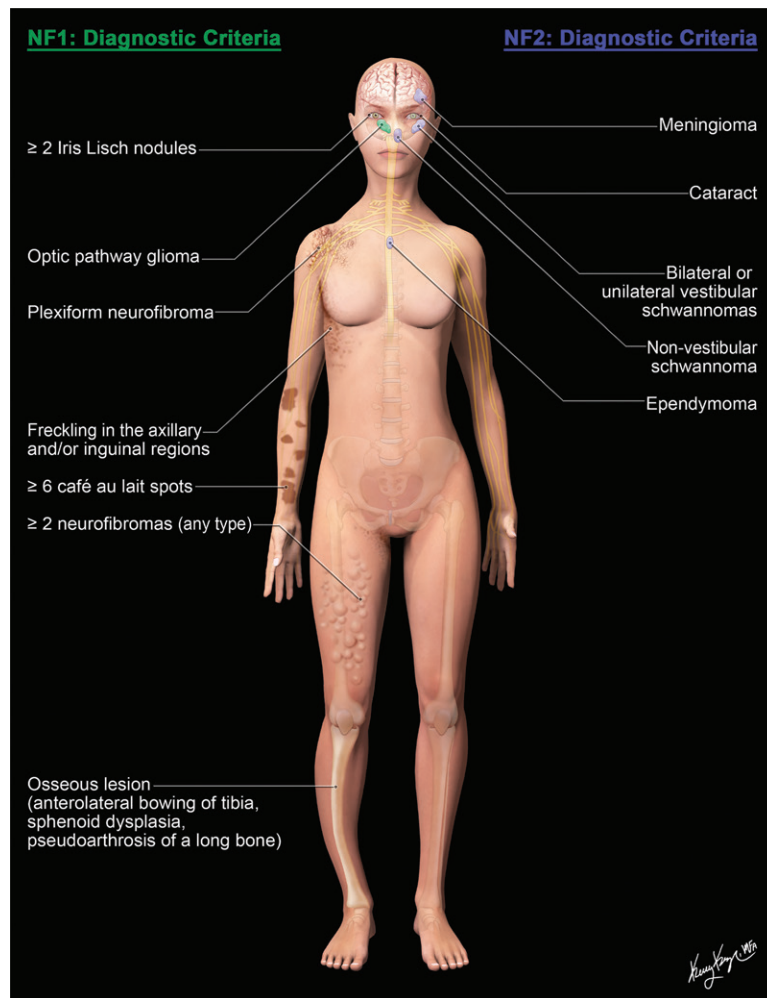


Figure 1. Key diagnostic features for NF1 and NF2.

Neurofibromatosis Type 2

Bilateral vestibular schwannomas were considered pathognomonic for NF2; however, subsequent studies demonstrated that this feature is not sufficient for NF2 diagnosis, as they can be associated with leucine zipperlike transcription regulator 1 (*LZTR1*) germline mutations (8). The Manchester diagnostic criteria for NF2 were updated in 2017, incorporating the facts that unilateral vestibular schwannoma may be due to *LZTR1* germline mutations rather than NF2 and that vestibular schwannomas are rarely seen with NF2 after the age of 70 years (Table 2) (Fig 1) (8).

NF1 Multisystem Manifestations

Cutaneous Manifestations

Various cutaneous manifestations are commonly seen with NF1, primarily café-au-lait macules, axillary and inguinal freckling, neurofibromas, and plexiform neurofibromas. Café-au-lait macules are benign, tan-brown pigmented, flat skin patches that occur in 99% of NF1 individuals (Figs 2, E1)

(9). They can be seen at birth and increase in size and number over time. Although commonly seen, they are nonspecific and can be seen in 10% of the general population (5). However, the presence of six or more café-au-lait macules is highly predictive of NF1 (10). Axillary and inguinal freckling manifests as small clustered pigmented macules that occur in 90% of NF1 cases by the age of 7 years (9). While these manifestations are benign, they can be a cosmetic concern, for which laser therapy may be considered (5,11).

Dermal and subcutaneous neurofibromas are benign peripheral nerve sheath tumors (PNSTs), occurring in approximately 60% of NF1 patients (5). They result from proliferation of spindle cells, Schwann cells, mast cells, and vascular components. Neurofibromas can arise anywhere in the body along the nerves. On the skin, they manifest as fleshy, pink-to-brown, pedunculated papulonodules in young adults (9). Over time, they may grow and increase in number.

At US, they manifest as well-defined oval hypoechoic masses contiguous with peripheral nerves, often demonstrating posterior acoustic

Table 2: Revised Manchester Criteria for NF2

The presence of any one of the following criteria suggests the diagnosis of NF2:

- Bilateral vestibular schwannomas before age 70 years
- Unilateral vestibular schwannoma before age 70 years and a first-degree relative with NF2
- Any two of the following tumor types: meningioma, nonvestibular schwannoma, ependymoma, cataract; and
 - First-degree relative with NF2 or
 - Unilateral vestibular schwannoma and negative result at *LZTR1* testing
- Multiple meningiomas and
 - Unilateral vestibular schwannoma or
 - Any two of the following: nonvestibular schwannoma, ependymoma, cataract
- Constitutional or mosaic pathogenic *NF2* gene mutation in blood or by identification of an identical mutation from two separate tumors in the same individual

Source.—Adapted, with permission, from reference 8.



Figure 2. Café-au-lait macules in a 6-year-old girl with NF1. Photograph shows multiple café-au-lait macules on the torso. At least six macules are seen, which is highly predictive of NF1. (See also Fig E1.)

enhancement. At color Doppler imaging, internal flow is expected, although they are generally hypovascular (12). At CT, they manifest as soft-tissue masses with low attenuation (Table 3) (13). At MRI, neurofibromas may demonstrate the target sign (hyperintense peripheral rim and hypointense central fibrous component) on T2-weighted images and central enhancement (14).

Although malignant transformation in cutaneous neurofibromas is exceedingly rare, they can be a cosmetic concern and cause irritation. Surgical removal, laser ablation, and electrodesiccation are treatment options (11,15).

Plexiform neurofibromas are complex deep or superficial masses that arise from peripheral nerve sheaths, occurring in 40%–50% of patients with NF1 (16). They appear as thickened firm masses or nodules that may deeply infiltrate structures, causing disfigurement and dysfunction. At MRI, they manifest as multinodular confluent masses with mass effect on surrounding structures and multiple target signs on T2-weighted images (Figs 3, E2) (14). Surgical removal is often difficult (11). Targeted therapy with mammalian target of rapamycin (mTOR) inhibitors or mitogen-activated protein kinase kinase (MEK) inhibitors may be helpful but is not curative (3,15).

Owing to the moderately high risk of developing breast cancer, patients with NF1 should undergo screening mammography starting at the age of 30 years (17). However, the presence of cutaneous neurofibromas may pose a diagnostic challenge for mammographic interpretation (18).

Ophthalmic Manifestations

Lisch nodules are the most common clinical feature of NF1 (19). They are benign iris hamartomas composed of pigmented cells, mast cells, and fibroblasts (20). They are identified as pigmented flat or slightly elevated lesions at slit-lamp examination (Fig 4). They are helpful for earlier diagnosis, since they manifest before neurofibromas and are NF1 specific, unlike café-au-lait macules. No specific treatment is needed (9).

Sphenoid wing dysplasia is a hallmark skull abnormality in NF1 patients attributed to mesodermal dysplasia, occurring in more than 10% of cases (14,21). It manifests as greater and lesser sphenoid wing hypoplasia, which is indicated by the bare orbit sign (absence of the innominate line) at plain radiography and CT (14,22). Associated widening of the middle cranial fossa (Fig 5), widening of the orbital fissures, and flattening of the posterior orbit may result in pulsatile exophthalmos, incomplete lid closure, buphthalmos, and vision loss (22). In severe cases, meningocele and meningoencephalocele can be seen. Over half of these patients have an associated plexiform tumor that disrupts bone remodeling (22). Multidisciplinary surgical management is crucial in these cases.

Central Nervous System Manifestations

Central nervous system (CNS) manifestations are one of the most common findings in NF1 (23). Various clinical manifestations include learning and language difficulties, inattention,

Table 3: Imaging Features of Common NF1-related Manifestations

Common Manifestations	Commonly Used Imaging Modality or Modalities	Imaging Features
Neurofibromas	US, CT, MRI	US: well-defined oval hypoechoic masses contiguous with peripheral nerves CT: soft-tissue masses with low attenuation MRI: target sign (T2 hyperintense peripheral rim and hypointense central component), enhancement of central component
Plexiform neurofibromas	MRI	Multinodular confluent masses with multiple target signs and mass effect on surrounding structures
Malignant PNSTs	MRI	Similar to plexiform neurofibromas with suggestive features: large size, peripheral enhancement pattern, perilesion edemalike zone, intratumor cystic changes
Sphenoid wing dysplasia	CT, MRI	Hypoplastic sphenoid wing, widened middle cranial fossa, flattened posterior orbit, possible meningocele and meningoencephalocele
Focal areas of signal intensity (FASIs)	MRI	Focal or diffuse T2 hyperintensity in the basal ganglia, cerebellum, or brainstem without enhancement or mass effect
Optic pathway glioma	MRI	T1-hypointense, T2-hyperintense, and homogeneously enhancing enlargement of the optic nerve sheath complex
Non-optic pathway glioma	MRI	T1-hypointense or -isointense, T2-hyperintense, and variably enhancing intraparenchymal lesion, usually in the brainstem or cerebellum; may cause obstructive hydrocephalus
Dural ectasia, meningocele	CT, MRI	Well-circumscribed paravertebral mass following CSF signal intensity, often in the anterior or anterolateral aspect of the vertebral column
Interstitial lung disease	CT	Bilateral, symmetric, basal-predominant linear and ground-glass opacities; apical-predominant cysts and centrilobular nodules
GIST	CT, MRI	Submucosal bowel wall tumor with an endophytic, exophytic, or combined growth pattern
Pheochromocytoma or paraganglioma	CT, MRI	CT: well-circumscribed homogeneously enhancing adrenal gland mass (pheochromocytoma) or extra-adrenal mass (paraganglioma) MRI: often T2 hyperintense; possible T2 intermediate signal intensity due to hemorrhage, cystic changes, or myxoid degeneration
Rhabdomyosarcoma	CT, MRI	Heterogeneous enhancement with local invasion of organs and destruction of bone
Scoliosis	XR, CT	Lateral spinal curvature with sharply angulated segments of four to six vertebrae
Bone dysplasia	XR, CT	Posterior vertebral body scalloping; thinning of the pedicles, transverse processes, laminae; neural foramen enlargement; rib deformities; anterolateral tibial bowing, fracture, and pseudoarthrosis
Nonossifying fibromas	XR, CT, MRI	Slightly expansile cortically based lesions in the metaphysis of long bones with thin sclerotic borders and narrow zone of transition
Vascular dysplasia	US, CT, MRI	Narrowing and aneurysmal dilatation of various arteries (eg, renal artery, abdominal aorta, and terminal internal carotid artery)

Note.—CSF = cerebrospinal fluid, GIST = gastrointestinal stromal tumor, XR = radiography.

impulsivity, epilepsy, headaches, and neurologic symptoms. CNS tumors occur in 1%–3% of patients with NF1 and are significant contributors to mortality (21,24).

Focal Areas of Signal Intensity.—Focal areas of signal intensity (FASIs) are common MRI findings, occurring in approximately 70% of NF1 cases (23,25). Temporal change in number and size is noted, appearing by the age of 3 years, followed by a size decrease after the age of 20

years (26). Several studies have explored their association with cognitive impairment, with FASIs localized in the thalamus and cerebellum found to be strongly correlated (27–29). However, the underlying cause of cognitive impairment is complex, with disruption of the brain microstructure and with FASIs likely being a by-product of this process (22,30). Histologically, they demonstrate abnormally increased white matter volume related to spongiform myelopathy and myelin vacuolization (22).

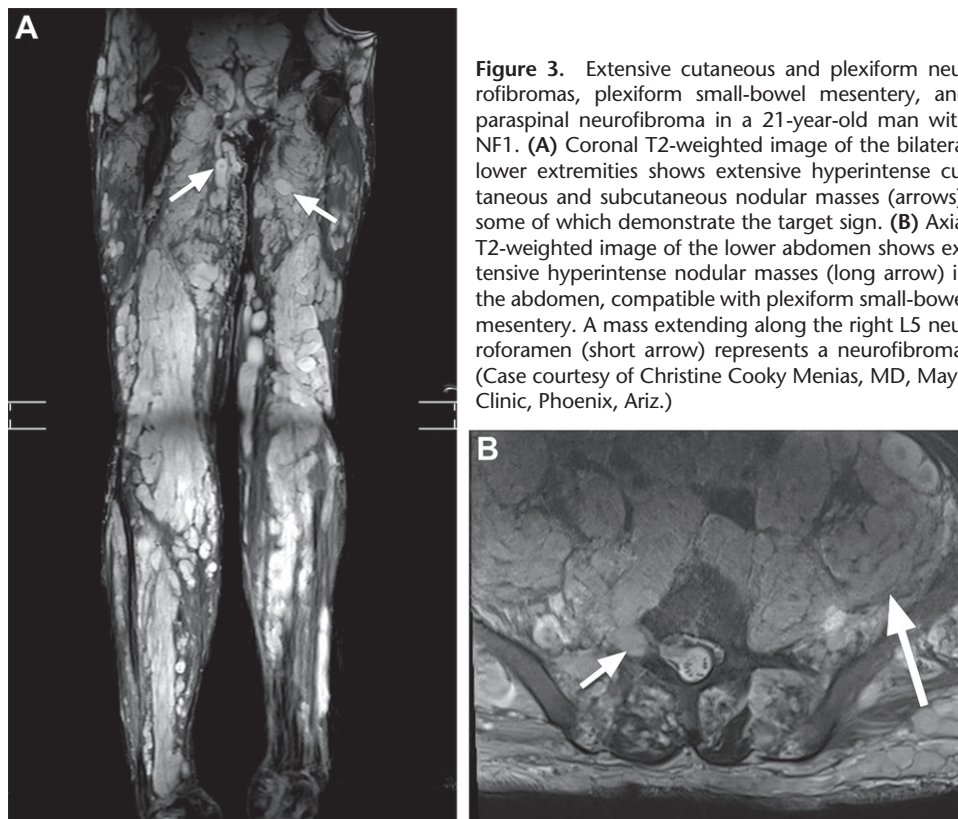


Figure 3. Extensive cutaneous and plexiform neurofibromas, plexiform small-bowel mesentery, and paraspinal neurofibroma in a 21-year-old man with NF1. (A) Coronal T2-weighted image of the bilateral lower extremities shows extensive hyperintense cutaneous and subcutaneous nodular masses (arrows), some of which demonstrate the target sign. (B) Axial T2-weighted image of the lower abdomen shows extensive hyperintense nodular masses (long arrow) in the abdomen, compatible with plexiform small-bowel mesentery. A mass extending along the right L5 neuroforamen (short arrow) represents a neurofibroma. (Case courtesy of Christine Cooky Menias, MD, Mayo Clinic, Phoenix, Ariz.)

At MRI, FASIs demonstrate focal or diffuse hyperintensity in the basal ganglia, cerebellum, or brainstem at T2-weighted imaging and fluid-attenuated inversion-recovery (FLAIR) imaging, relative to the brain (Fig 6) (25). They generally exhibit isointensity or mild hyperintensity at T1-weighted imaging, no enhancement, and no mass effect. At MR spectroscopy, they demonstrate preserved *N*-acetylaspartate level, unlike gliomas (22). FASIs may be bilateral and symmetric, especially when involving the basal ganglia (25).

Optic Pathway Gliomas.—Optic pathway gliomas are the most common CNS tumors in NF1, occurring in approximately 15%–20% of cases (31). These gliomas can involve any portion of the optic pathway. Although they demonstrate indolent behavior, up to 50% of these tumors can cause symptoms, such as poor visual acuity, optic atrophy, visual field defects, hypothalamic dysfunction, and papilledema (1,26,32). They tend to manifest in young children with a median age of approximately 4 years (33). Histologically, they are often distinguished as pilocytic astrocytomas; however, pathologic structure has little influence on their management (34).

At MRI, they demonstrate enlargement of the optic nerve sheath complex, which is hypointense on T1-weighted images and hyperintense on T2-weighted images with variable enhancement (com-

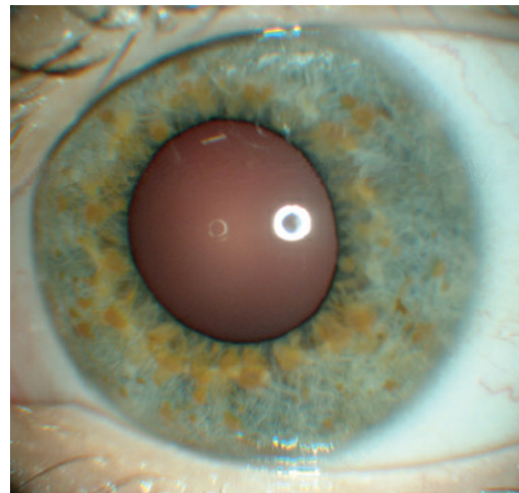


Figure 4. Lisch nodules in a 14-year-old boy with NF1. Slit-lamp photograph of the left eye shows numerous yellow-brown Lisch nodules.

pared with the brain) (Fig 7) (26). Although most of these tumors may regress without treatment, chemotherapeutic agents are used when there is progressive vision loss. Medications that block RAS and mammalian target of rapamycin (mTOR) pathways are also options (1). Surgery should be considered for severe symptoms and large tumors (≥ 5 cm) (3,23). Radiation therapy is generally spared for unresectable or metastatic tumors owing to the risk of developing secondary neoplasms (3).

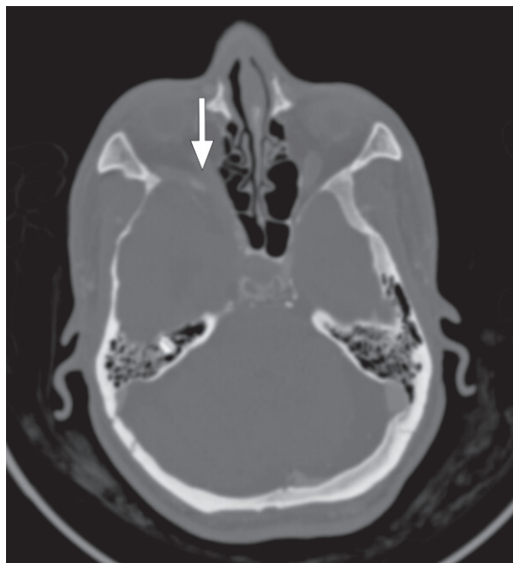


Figure 5. Sphenoid wing dysplasia in a 36-year-old woman with NF1. Axial CT image of the head (bone window) shows an absent right sphenoid wing, a bone defect (arrow) in the posterior aspect of the orbit, and expansion of the right middle cranial fossa.

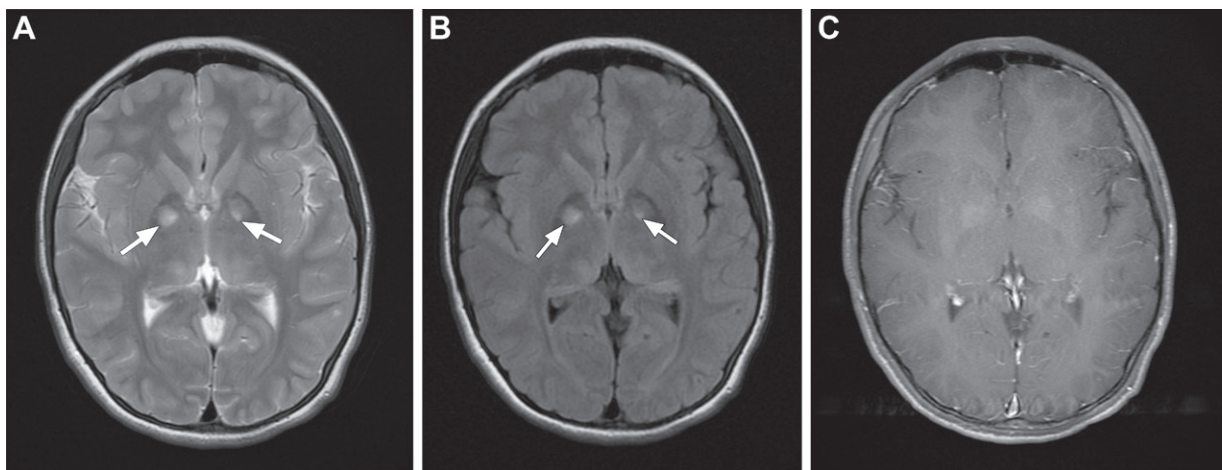


Figure 6. FASIs in a 13-year-old boy with NF1. (A) Axial T2-weighted image of the brain shows bilateral hyperintense foci (arrows) in the lentiform nuclei. (B) Axial T1-weighted image shows corresponding mildly hyperintense foci (arrows). (C) Axial contrast-enhanced T1-weighted image shows no enhancement of the foci, consistent with FASIs.

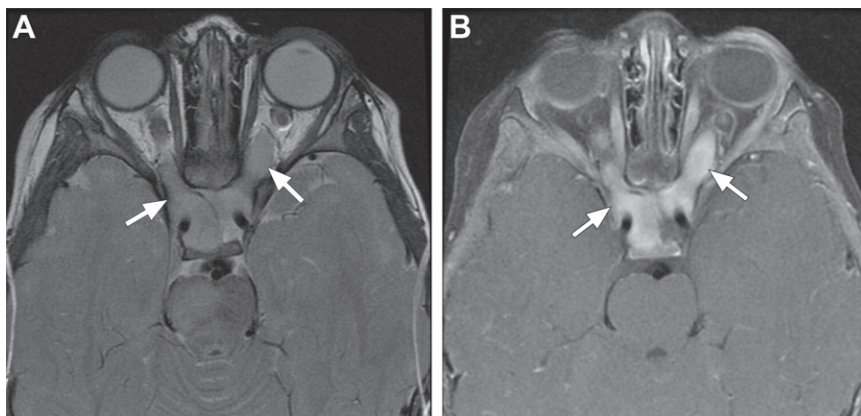


Figure 7. Optic pathway glioma in an 18-month-old girl with NF1. (A) Axial T2-weighted image of the brain and orbits shows central hyperintensity (arrows) along the enlarged optic nerves extending to the optic chiasm. (B) Axial contrast-enhanced T1-weighted image shows homogeneous enhancement of the tumor (arrows).

Non-Optic Pathway Intracranial Gliomas.— Most non-optic pathway intracranial gliomas associated with NF1 are low-grade astrocytomas, most commonly pilocytic astrocytomas. They

occur in approximately 1%–2% of NF1 patients (31). Unlike non-NF1-related gliomas, NF1-related gliomas are often asymptomatic with an indolent course (35). However, symptoms may

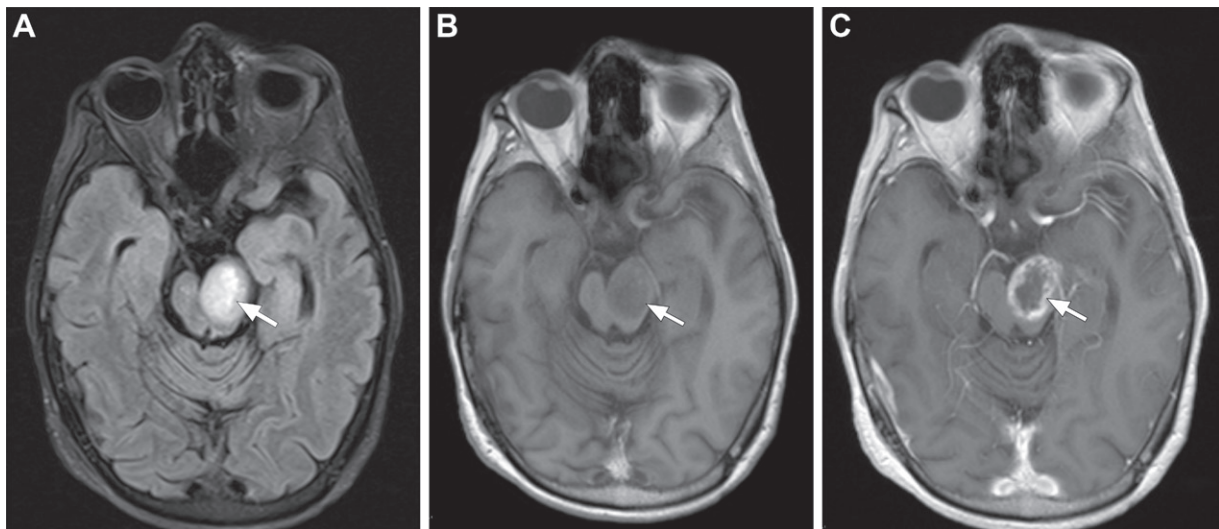


Figure 8. Non-optic pathway intracranial glioma in a 34-year-old man with NF1 undergoing radiation therapy. (A) Axial fluid-attenuated inversion-recovery (FLAIR) image of the brain shows a hyperintense infiltrative expansile mass (arrow) involving the pons extending into the left cerebral peduncle. (B) On an axial T1-weighted image, the mass (arrow) is isointense to gray matter. (C) Axial contrast-enhanced T1-weighted image shows associated peripheral enhancement (arrow) of the mass.

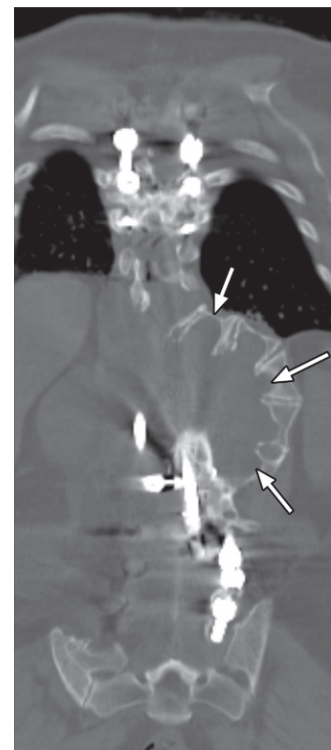
include headaches, seizures, and ataxia (35,36). These gliomas are usually located in the brainstem or posterior fossa (26). With tectal involvement, obstructive hydrocephalus may occur. Rarely, intramedullary spinal gliomas can be seen (26).

At MRI, they demonstrate hypo- or isointensity on T1-weighted images and hyperintensity on T2-weighted images with variable enhancement (Fig 8). Gliomas are distinguished from FASIs by the presence of mass effect, their T1 and T2 characteristics, contrast enhancement, and evolution over time (20,35). MR spectroscopy can also help differentiate these from FASIs, as gliomas demonstrate decreased or absent *N*-acetylaspartate, increased choline, and decreased creatine levels (22). Rarely, multiple intracranial gliomas may be present; thus, a search for additional optic pathway or non-optic pathway gliomas is prompted (37).

Most brainstem gliomas do not require treatment apart from shunting for hydrocephalus. When gliomas are symptomatic or with disease progression, surgical resection, radiation therapy, or chemotherapy may be warranted (20). Targeted therapies, such as those targeting the RAS/mitogen-activated protein kinase (MAPK) pathway, are under investigation (38).

Dural Ectasia and Meningocele.—Dural ectasia and meningocele occur along the same spectrum, occurring in 70%–80% of NF1 patients (Figs 9–11) (22,39,40). Dural ectasia represents focal dilatation of the dural sac, which may be related to underlying bony weakness (14). Meningocele occurs along the course of nerve roots, at the anterior or anterolateral aspect of

Figure 9. Severe scoliosis and extensive vertebral body scalloping in a 44-year-old woman with NF1. Coronal CT image of the thoracolumbar spine (bone window) shows severe S-shaped scoliosis of the thoracolumbar spine with bilateral Harrington rods. The extensive vertebral body scalloping (arrows) is likely associated with dural ectasia and meningocele.



the vertebral column, and in the thoracic spine as a result of pressure differences between the thorax and subarachnoid space (13).

Both are typically asymptomatic and small. They are well-circumscribed low-attenuation paravertebral masses at CT, with corresponding cerebrospinal fluid signal intensity at MRI (13,26). At CT myelography, intrathecally injected contrast material fills these spaces. They are often associated with vertebral defects and spine scoliosis.



Figure 10. Multiple meningoceles in a 36-year-old woman with NF1. Sagittal T2-weighted image of the cervical spine shows hyperintense focal outpouchings (arrows) through multiple left cervical neuroforamina.

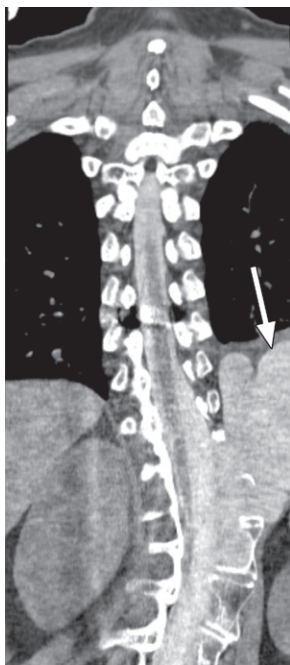


Figure 11. Large meningocele and scoliosis in a 42-year-old woman with NF1. Coronal CT myelogram of the thoracic spine shows a large meningocele (arrow) extending from the left neural foramen at the T11 level into the upper left posterior abdominal cavity with erosions of the T11 vertebral body and left-sided posterior elements. Levoscoliotic curvature of the thoracolumbar spine is present.

Nerve Sheath Tumors.—In addition to cutaneous involvement, neurofibromas and plexiform neurofibromas may involve the spinal cord and spinal nerve roots with the aforementioned imaging features (Figs 12, 13, E3, E4). Patients may be asymptomatic or have neurologic deficits due to spinal cord compression, which is typically mild and occurs at the levels of C2 and C3 (1,20). Paraspinal neurofibromas can manifest as solitary or multiple dumbbell-shaped masses with paraspinal or intradural extramedullary components, associated with enlarged neural foramina, scoliosis, vertebral dysplasia, and possible spinal cord compression (26). Surgical resection should be considered for patients with progressive neurologic deficits (20).

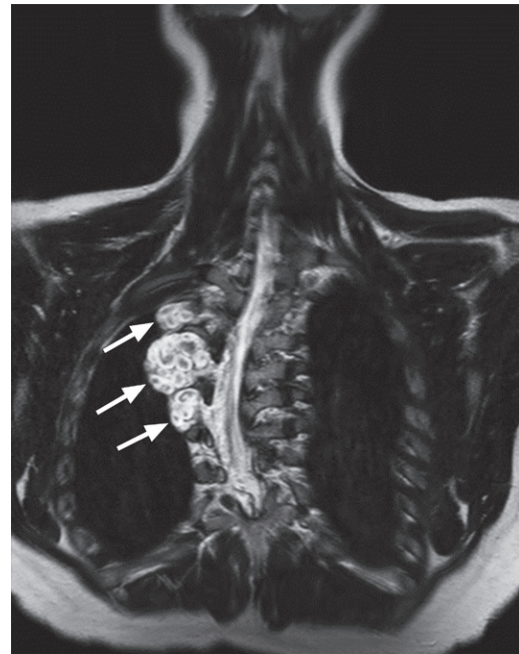


Figure 12. Multiple paraspinal neurofibromas in a 13-year-old boy with NF1. Coronal T2-weighted image of the chest shows multilevel hyperintense masses (arrows) with the target sign extending along the right thoracic neuroforamina. Note that the spinal dextrocurvature is centered at the level of the neurofibromas.

Malignant PNSTs.—Malignant PNSTs are highly malignant soft-tissue sarcomas that can arise from any neurofibroma. They can infiltrate surrounding soft tissue, cause peritumor edema, and are often located in the extremities and trunk (41). Patients may present with persistent pain, rapid growth or new hard texture, and new or unexplained neurologic deficit associated with a neurofibroma (1). Malignant PNSTs are key contributors to mortality in patients with NF1 (24).

At MRI, malignant degeneration is suggested by heterogeneous signal intensity on T1-weighted images. Four imaging features can help differentiate malignant PNST from benign neurofibroma at MRI: large dimension of the mass, peripheral enhancement pattern, perilesion edema-like zone, and intratumor cystic changes (Figs 14, E5) (42). The presence of two or more of these features has sensitivity of 61% and specificity of 90% for indicating a malignant PNST (42). Additional features that favor malignant PNST include ill-defined margins, intratumor lobulation, and adjacent bone destruction (41). At fluorine 18 (^{18}F) fluorodeoxyglucose (FDG) PET/CT, malignant PNST generally demonstrates a maximum standardized uptake value (SUV_{max}) greater than 3.5, while benign lesions demonstrate an SUV_{max} less than 2.5, with some overlap (43).

Surgical resection is the primary treatment. Unfortunately, recurrence is common even with negative surgical margins (44). Radiation therapy

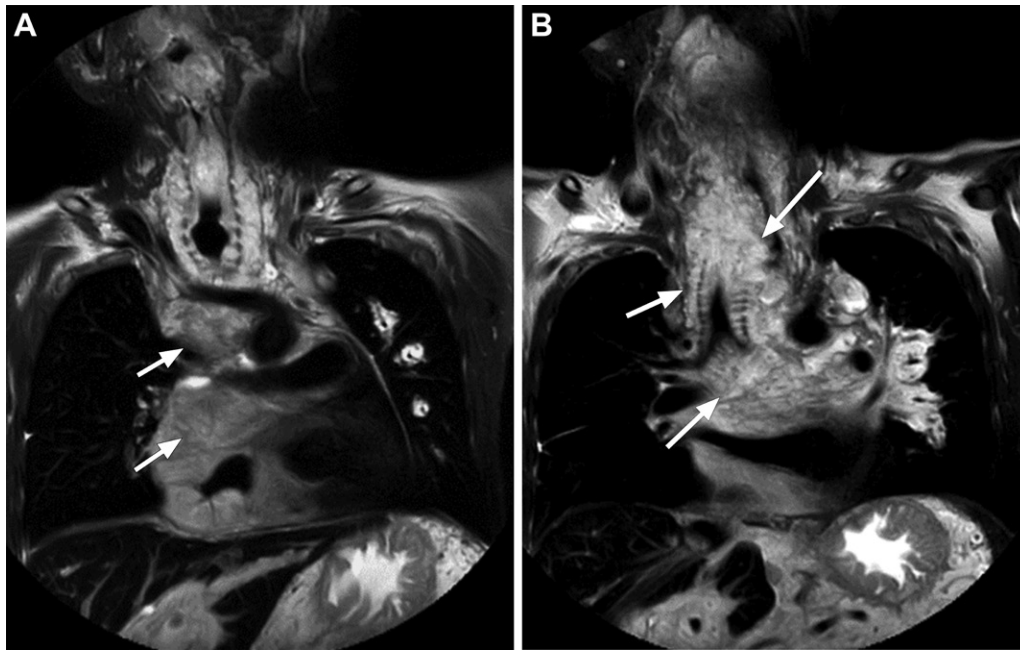


Figure 13. Extensive plexiform neurofibromas with tracheobronchial, cardiac, and posterior mediastinal involvement in a 16-year-old adolescent boy with NF1. Coronal T2-weighted images of the chest show numerous hyperintense nodular masses (arrows) with the target sign with tracheobronchial, cardiac, and posterior mediastinal involvement.

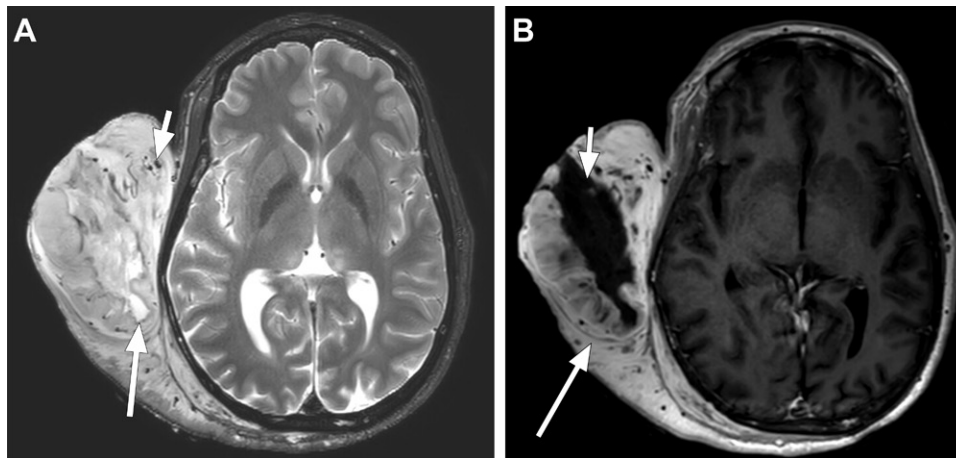


Figure 14. Malignant PNST in a 61-year-old man with NF1. (A) Axial T2-weighted image of the brain shows a large exophytic mass centered in the right occipital scalp with internal cystic changes (long arrow), flow voids (short arrow), and heterogeneous signal intensity. (B) Axial contrast-enhanced T1-weighted image shows avid peripheral enhancement (long arrow) of the mass and internal cystic changes (short arrow), suggestive of malignant PNST.

and chemotherapy can be used for extensive or residual disease (1). Therapies such as epidermal growth factor receptor inhibitors and tyrosine kinase inhibitors are under investigation (45).

Pulmonary Manifestations

NF1-related pulmonary manifestations, including interstitial lung disease, cyst or bulla formation, and pulmonary hypertension, occur in 10%–20% of adults with NF1 (46,47). In severe cases, the cystic disease can cause respiratory failure, spontaneous pneumothorax, or pulmonary hyper-

tension. At pathologic analysis, NF1-associated interstitial lung disease is similar to diseases with interstitial fibrosis, ultimately resulting in destruction of the alveoli (47).

At CT, this manifests as linear and ground-glass opacities that are bilateral, symmetric, and basal predominant. Apical-predominant cysts (Fig 15) and centrilobular nodules are also seen. The cysts become clustered in advanced stages, which can be mischaracterized as centrilobular emphysema (47). There are no specific treatments for these manifestations.

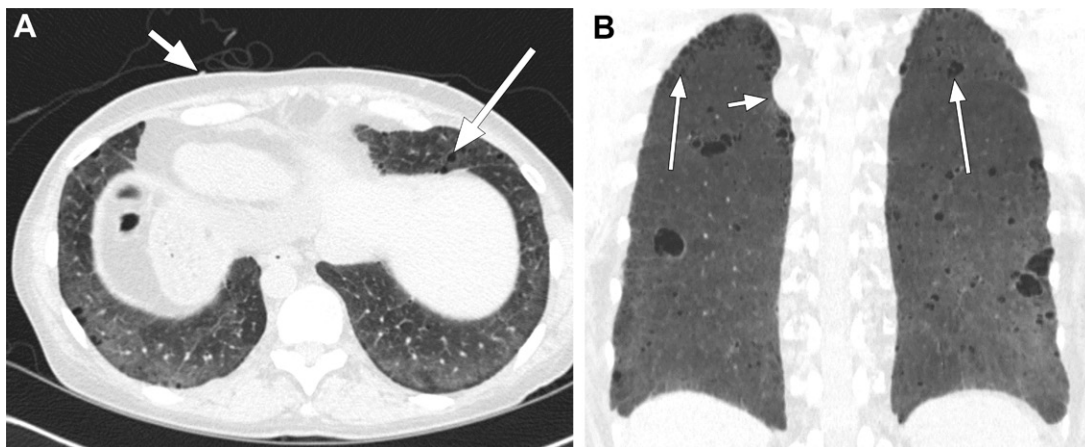


Figure 15. Interstitial lung disease, pulmonary cysts, cutaneous neurofibroma, and paraspinal neurofibroma in a 51-year-old woman with NF1. **(A)** Axial CT image (lung window) shows ground-glass opacities in the lung bases with subpleural sparing, compatible with a nonspecific interstitial pneumonia pattern of interstitial lung disease. Scattered pulmonary cysts (long arrow) and a cutaneous neurofibroma (short arrow) are noted. **(B)** Coronal minimum intensity projection CT image shows the upper lobe–predominant pulmonary cysts (long arrows). A paraspinal neurofibroma is present (short arrow).

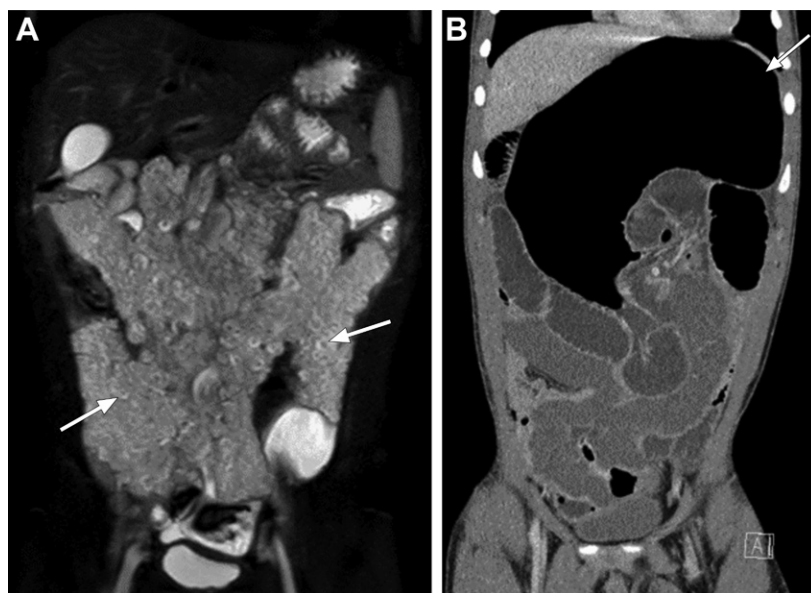


Figure 16. Plexiform small-bowel mesentery in an 11-year-old boy with NF1. **(A)** Coronal T2-weighted image of the abdomen shows numerous hyperintense nodular masses (arrows) with the target sign throughout the small-bowel mesentery. **(B)** Coronal CT image of the abdomen with intravenous contrast material 3 years later shows dilated loops of bowel, with the largest one (arrow) representing the stomach. The plexiform small-bowel mesentery served as a lead point, causing segmental volvulus.

Abdominopelvic Manifestations

The various NF1-associated intra-abdominal neoplasms can be categorized by their cellular origin: neurogenic neoplasms, interstitial cells of Cajal neoplasms, neuroendocrine neoplasms, and embryonal neoplasms. Approximately 5%–25% of individuals with NF1 develop intra-abdominal neoplasms (44).

Neurogenic Neoplasms.—Neurofibromas are the most common NF1-related abdominopelvic neoplasm. They often manifest in the retroperitoneum and pelvis along the distribution of the lumbosacral plexus. They may also involve any portion of the gastrointestinal tract or mesentery owing to the presence of a rich supply of nerve tissue. When a large conglomeration of neuro-

fibromas is seen, it is considered a plexiform neurofibroma. Nonspecific symptoms related to mass effect may include pain, palpable abdominal mass, bowel obstruction, and gastrointestinal bleeding (44). Rapid growth, pain, and new neurologic deficit should alert one to possible malignant transformation into malignant PNST.

At CT, neurofibromas manifest as well-defined mildly enhancing masses, sometimes appearing cystic (12). When the bowel wall nerve plexus is involved, neurofibromas can manifest as circumferential masslike wall thickening with or without obstruction. Plexiform neurofibromas appear as large infiltrating masses (Fig 16) (13). They can be hypervascular or hypovascular. Vascular narrowing may occur, which can cause bowel ischemia (13). Surgical resection is considered for symptomatic

or rapidly enlarging plexiform neurofibromas and malignant PNSTs.

Interstitial Cells of Cajal Neoplasms.—Solitary and multifocal gastrointestinal stromal tumors (GISTs) can occur in up to 25% of individuals with NF1 (48), although the majority (53%) are asymptomatic (49). GISTs can manifest with abdominal pain, gastrointestinal bleeding, or bowel obstruction. They often manifest in the small bowel and occur in more than one gastrointestinal site.

At CT and MRI, GISTs are submucosal bowel wall masses with an endophytic, exophytic, or mixed growth pattern (Fig 17). They typically enhance, although enhancement can be heterogeneous in larger tumors owing to necrosis (12). When symptomatic, they are surgically resected (44).

Neuroendocrine Neoplasms.—Pheochromocytomas are catecholamine-secreting tumors that arise from chromaffin cells of the sympathetic-adrenal system and occur in 1%–7% of individuals with NF1 (50). When functional, they can manifest with hypertension, headache, palpitations, and diaphoresis (44). A subset of pheochromocytomas occur extra-adrenally, which are called paragangliomas.

At CT, pheochromocytomas are typically well-circumscribed masses in the adrenal gland. They can be homogeneously enhancing, although when large (>3 cm) they often exhibit heterogeneity due to internal hemorrhage, necrosis, or cystic changes (12). At MRI, they classically exhibit T2 hyperintensity similar to that of CSF (lightbulb sign), although this is seen in only 11%–65% of cases (Fig 18) (12). Occasionally, they may demonstrate intermediate T2 signal intensity due to hemorrhage, cystic changes, or myxoid degeneration. When cystic, they appear with rim enhancement.

Iodine 123–metaiodobenzylguanidine (MIBG) scintigraphy can help detect functional lesions. Surgical resection is the mainstay of therapy, with chemotherapy or radiation therapy used when lesions are unresectable or large (44).

Neuroendocrine neoplasms tend to arise in the periampullary duodenum but can rarely occur in the pancreas (51). Somatostatinoma is the most common subtype and classically manifests with diarrhea, diabetes, dyspepsia, or cholelithiasis (44). At CT and MRI, it demonstrates hyperenhancement in the periampullary region with possible biliary obstruction and pancreatitis. When lesions are large (>2 cm) with poor differentiation, pancreaticoduodenectomy is warranted. When lesions are small (<2 cm), endoscopic resection can be considered (44).

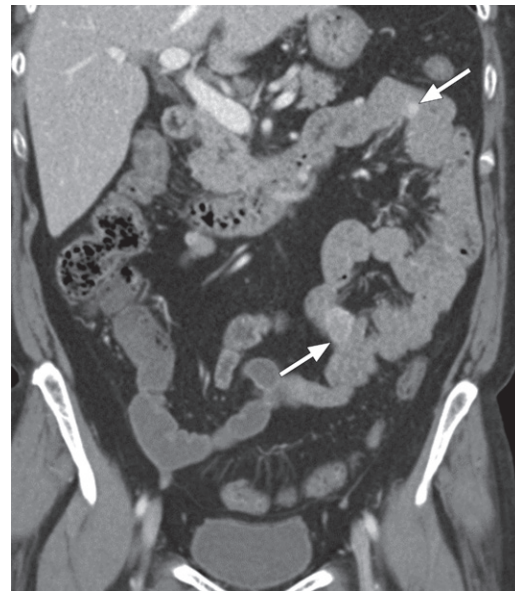


Figure 17. Multiple gastrointestinal stromal tumors (GISTs) in a 66-year-old woman with NF1. Coronal CT image of the abdomen with intravenous contrast material shows multiple avidly enhancing masses (arrows) along the small-bowel wall.

Embryonal Neoplasms.—Rhabdomyosarcoma is an aggressive soft-tissue tumor that occurs in up to 1% of pediatric patients with NF1 (52). At CT and MRI, rhabdomyosarcoma demonstrates heterogeneous enhancement due to necrosis and hemorrhage with local invasion of organs and destruction of bone (Fig 19) (12). Prominent flow voids can be seen. Treatment with chemotherapy, surgery, or radiation therapy is used (44,53).

Other Neoplasms.—Uterine leiomyomas are benign smooth muscle cell tumors that are uncommonly seen with NF1 (6). They may also involve the gastrointestinal and genitourinary tracts (6,54). They are mostly asymptomatic, although they may manifest with abnormal bleeding, complications with fertility, and pain (55).

At MRI, nondegenerated leiomyomas are well circumscribed and hypointense to myometrium on T2-weighted images, while cellular leiomyomas manifest with hyperintensity on T2-weighted images (56). Degenerated leiomyomas appear variably on T2-weighted images and contrast-enhanced images (56). Although both leiomyoma and leiomyosarcoma can demonstrate restricted diffusion, leiomyosarcoma tends to exhibit lower apparent diffusion coefficient (ADC) values (57). When leiomyomas are symptomatic, treatment options include hysterectomy, myomectomy, ablation, hormonal therapy, uterine artery embolization, and high-intensity focused US (56,58).

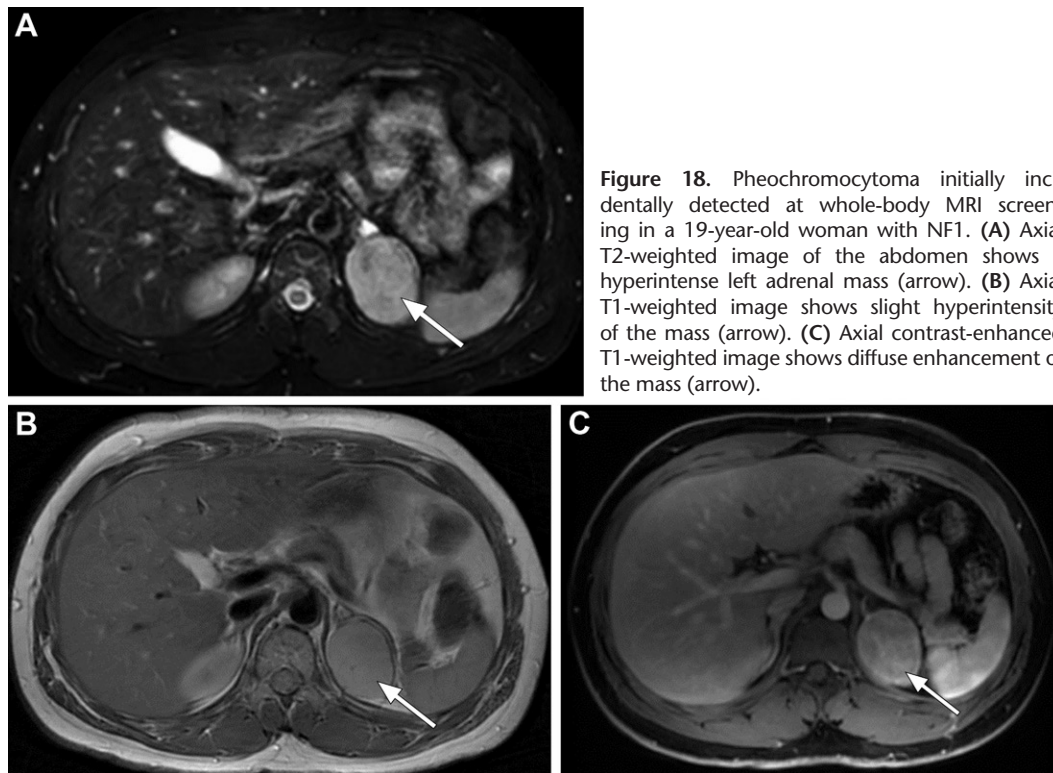


Figure 18. Pheochromocytoma initially incidentally detected at whole-body MRI screening in a 19-year-old woman with NF1. (A) Axial T2-weighted image of the abdomen shows a hyperintense left adrenal mass (arrow). (B) Axial T1-weighted image shows slight hyperintensity of the mass (arrow). (C) Axial contrast-enhanced T1-weighted image shows diffuse enhancement of the mass (arrow).

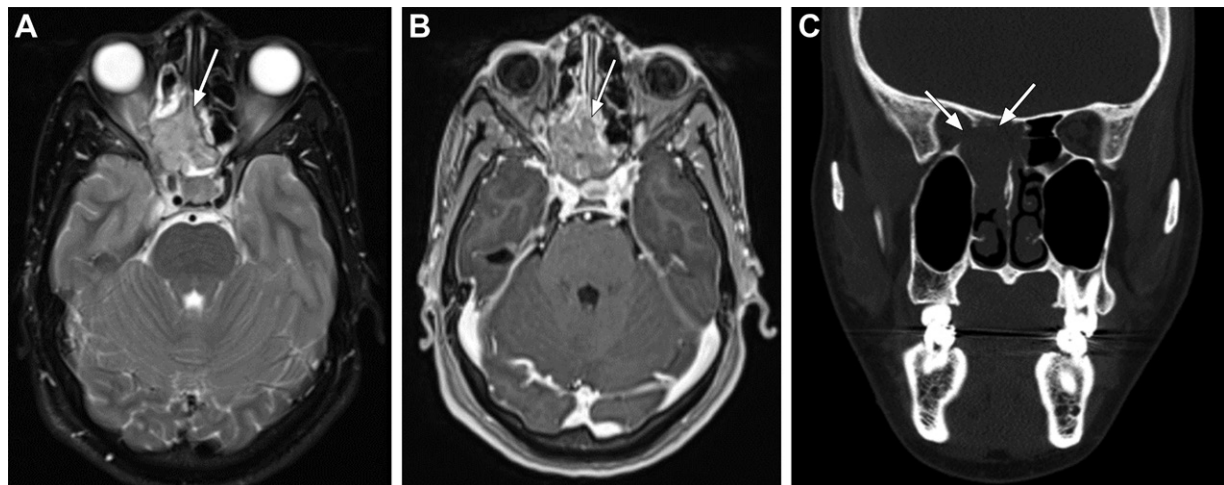


Figure 19. Sinus rhabdomyosarcoma in a 26-year-old woman with NF1. (A) Axial T2-weighted image of the head shows a heterogeneously hyperintense infiltrative mass (arrow) centered in the right posterior ethmoid air cells and extending into the right posterior orbit and left ethmoid air cells. (B) Axial contrast-enhanced T1-weighted image shows heterogeneous enhancement of the mass (arrow). (C) Coronal CT image of the face (bone window) shows associated osseous destruction (arrows).

Leiomyosarcoma is an aggressive soft-tissue sarcoma that is rarely seen with NF1 (59). It can occur in various locations, including the gastrointestinal tract, liver, and bladder (60). At MRI, leiomyosarcoma exhibits iso- or hypointensity on T1-weighted images and hyperintensity on T2-weighted images relative to muscle with heterogeneous enhancement. It may be associated with cystic changes. Surgical resection is the mainstay of treatment. Radiation therapy and chemotherapy can serve as neoadjuvant or adjuvant therapies (61).

Musculoskeletal Manifestations

Several skeletal abnormalities are commonly associated with NF1, including scoliosis, posterior vertebral scalloping, various bone dysplasias, and multiple nonossifying fibromas.

Scoliosis is the most common bone abnormality associated with NF1, occurring in 21% of patients (62). It often involves the lower cervical and upper thoracic spine (47). Nondystrophic scoliosis manifests similarly to childhood idiopathic scoliosis, while dystrophic scoliosis

manifests earlier and rapidly with a worse prognosis. Dystrophic scoliosis involves four to six vertebral bodies associated with vertebral scalloping, neuroforaminal widening, transverse process spindling, and rib penciling (14), which can potentially result in respiratory compromise (1). Surgery with spinal fusion is often required for correction. Nondystrophic scoliosis can be managed with bracing to prevent progression (15).

Vertebral body scalloping occurs as a result of dural ectasia, neurofibromas, or thoracic meningoceles and is possibly related to dural weakness (Fig 9) (26). Posterior vertebral scalloping is typically seen, although anterior and lateral scalloping have been reported (63). At imaging, posterior vertebral body scalloping exhibits exaggerated posterior vertebral concavity, with greater than 3-mm or 4-mm scalloping depth in the thoracic or lumbar spine, respectively (14,47).

There are various bone abnormalities related to mesodermal dysplasia and extrinsic pressure from neurofibromas. They manifest as thinning of the pedicles, transverse processes, and laminae; neural foraminal enlargement; and calvarial defects (Figs 20, E6) (14,64). Bone remodeling from adjacent neurofibromas can cause rib deformities (14). Additionally, involvement of the extremities can be seen, especially in the tibia and fibula, with anterolateral tibial bowing, fracture, and pseudarthrosis due to abnormal bone remodeling (Fig 21) (14). Bracing is recommended to prevent fracture, while bone grafting and fixation may be necessary to stabilize fractured bone (15).

Multiple nonossifying fibromas, also known as fibroxanthomas, are associated with NF1. They are asymptomatic and manifest as slightly expansile lesions in the metaphysis of long bones with thin sclerotic borders and a narrow zone of transition (14). Additionally, short stature involving the axial and appendicular skeleton and decreased bone mineral density are associated with NF1 (15,20).

Vascular Manifestations

NF1-associated vasculopathy can affect any arterial vessel, resulting in hypertension from renal artery stenosis, cerebrovascular events, or peripheral vascular insufficiency (15). The underlying pathogenesis is unclear, although arterial mesodermal dysplasia is thought to contribute to arterial lumen narrowing (20).

Renal artery stenosis is the most common vascular abnormality in individuals with NF1. The stenosis can be focal or multifocal and is often unilateral. At US, it demonstrates increased peak systolic velocity (>180 cm/sec) at the site of stenosis and increased renal-to-aortic ratio (>3.5)

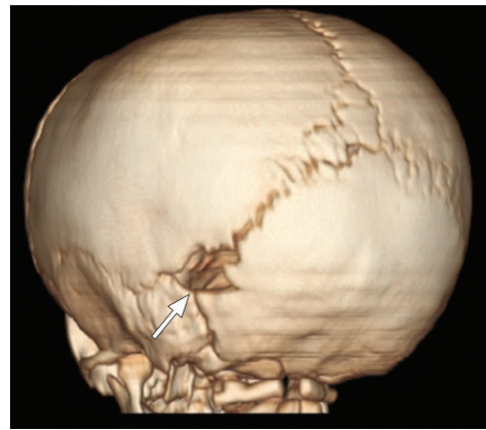


Figure 20. Lambdoid suture defect in a 1-year-old boy with NF1. Three-dimensional reconstructed image of the head shows a lambdoid suture defect (arrow).

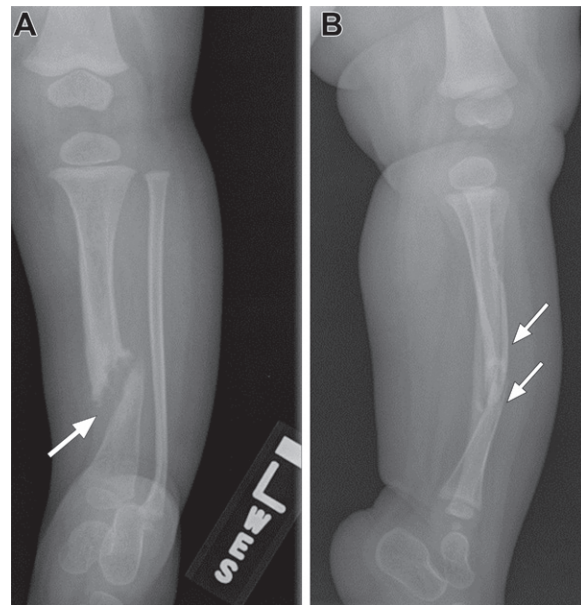


Figure 21. Tibial pseudarthrosis in a 12-month-old girl with NF1. Anteroposterior (A) and lateral (B) radiographs of the left tibia and fibula show progressive bowing with fracture (arrows) in the anterolateral tibia. The fibula also demonstrates anterolateral bowing.

(Figs 22, E7). At CT and MRI, smooth narrowing at the ostia can be seen along with narrowing of other vessels, including the mesenteric arteries and abdominal aorta (12). Management includes renal artery reimplantation, bypass, arterioplasty, and stenosis resection with reanastomosis.

Similarly, midaortic syndrome manifests with narrowing of the abdominal or distal descending thoracic aorta with stenoses of its branches, including the renal and mesenteric arteries (12) (Fig E8). This can be surgically managed with patch aortoplasty or bypass grafting.

Aside from renal artery stenosis, NF1-associated vasculopathy can manifest as cerebro-

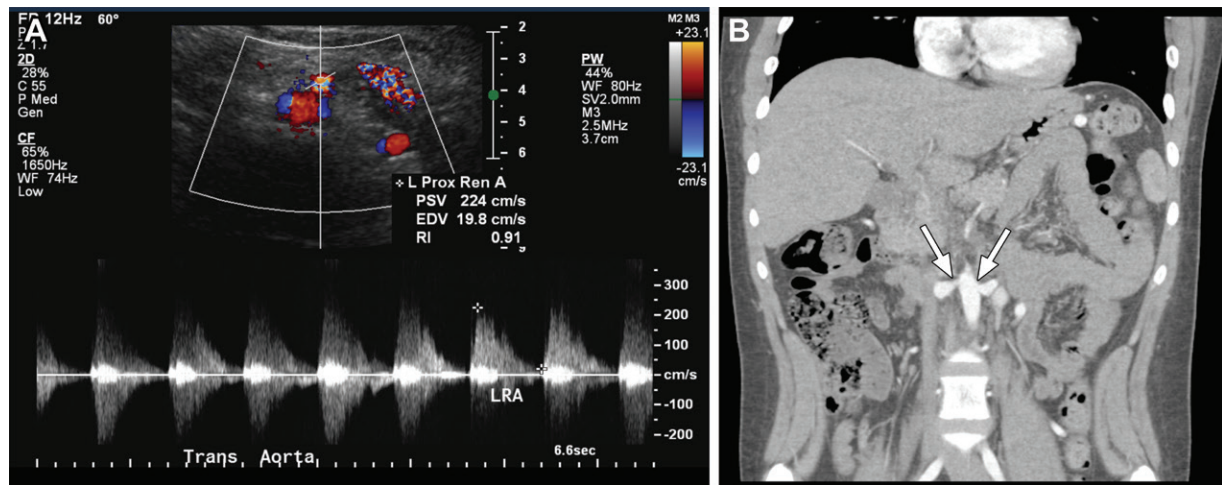


Figure 22. Bilateral renal artery stenoses in a 17-year-old adolescent boy with NF1. (A) Transverse US image of the left proximal renal artery shows increased peak systolic velocity (PSV). This finding and that in Figure E7 are suggestive of bilateral renal artery stenoses. (B) Coronal abdominal CT image with intravenous contrast material shows narrowing (arrows) of the proximal bilateral renal arteries.

Table 4: Imaging Features of Common NF2-related Manifestations		
Common Manifestation	Commonly Used Imaging Modality	Imaging Features
Schwannomas	MRI	Intracranial: T1-isointense or -hypointense, T2-hyperintense, and heterogeneously enhancing masses along cranial nerves (commonly involving the eighth cranial nerve) Spinal: intradural extramedullary masses (commonly at the level of C1)
Meningiomas	MRI	Intracranial: dural-based T1-isointense, T2-isointense, and homogeneously enhancing masses Spinal: intradural extramedullary T1-isointense, T2-isointense, and homogeneously enhancing masses
Ependymomas	MRI	Intracranial or spinal: intramedullary T1-isointense or slightly hyperintense and T2-hyperintense masses in the upper cervical cord and brainstem; homogeneously enhancing masses resemble a string of pearls; hemosiderin cap in the superior and inferior aspects

vascular disease with stenosis or occlusion of the internal carotid, middle cerebral, or anterior cerebral artery. Moyamoya disease, aneurysm, and arteriovenous malformation can also occur. In moyamoya disease, the terminal internal carotid artery or proximal portions of the anterior or middle cerebral artery are often obstructed and associated with collateral vessels (26). Moyamoya disease is typically treated with revascularization (15).

NF2 Manifestations

Unlike NF1, NF2 often manifests clinically in early adulthood with symptoms related to vestibular schwannomas (4). Early age of symptom onset and presence of intracranial meningiomas at diagnosis are associated with increased mortality (65). Key NF2 manifestations include schwannomas, meningiomas, and ependymomas (Table 4).

Cutaneous Manifestations

Cutaneous manifestations in NF2 are subtler than in NF1. Approximately 70% of patients with NF2 have cutaneous findings; however, only 10% have more than 10 cutaneous findings (66). Various NF2-related cutaneous manifestations include café-au-lait patches, cutaneous schwannoma plaque lesions, subcutaneous schwannomas, and rarely cutaneous neurofibromas.

Plaque lesions are the most common cutaneous feature, manifesting as slightly raised and pigmented lesions, often with excess hair (66). Individuals with NF2 generally have fewer café-au-lait patches (often one to three) than individuals with NF1 (1). As in NF1, troublesome neurofibromas can be removed surgically.

Ophthalmic Manifestations

Individuals with NF2 commonly have impaired vision. This may be secondary to presenile cataracts

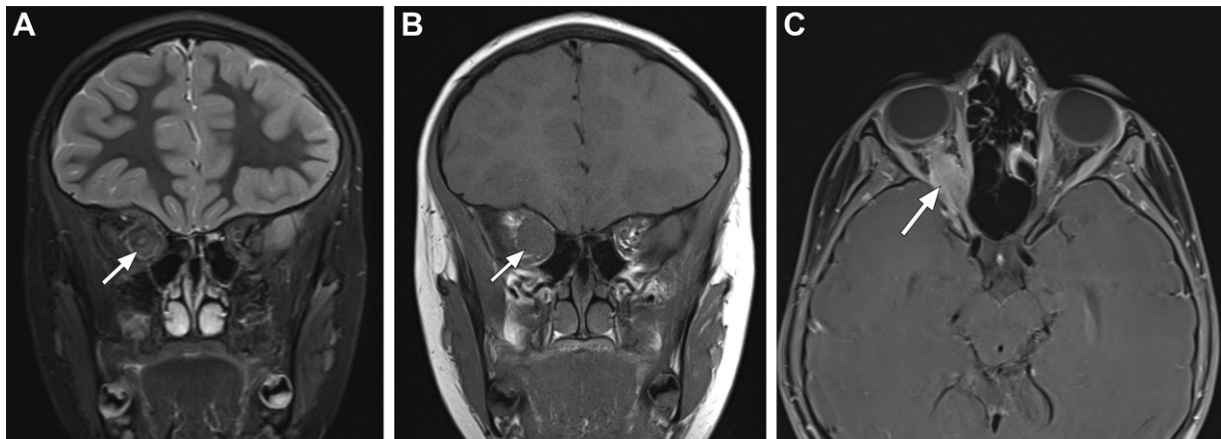


Figure 23. Optic nerve meningioma in a 6-year-old girl with NF2. (A) Coronal T2-weighted image of the orbits shows a right posterior intraorbital optic nerve sheath mass (arrow) that is hypointense to the optic nerve. The right optic nerve appears smaller than the left optic nerve. (B) Coronal T1-weighted image shows that the mass (arrow) is isointense to the optic nerve. (C) Axial contrast-enhanced T1-weighted image shows homogeneous enhancement of the optic nerve meningioma (arrow).

(60%–80%), epiretinal membranes, optic nerve meningiomas (Fig 23), disk gliomas, or retinal hamartomas (65,67). Oculomotor deficits, papilledema, and optic atrophy may manifest with intracranial tumors (67). Treatment is tailored to the pathologic condition and clinical manifestation (65).

CNS Manifestations

Schwannomas.—Schwannomas are benign tumors that arise from peripheral nerve sheaths and are the most common tumors occurring in NF2. They frequently involve the vestibular branch of the eighth cranial nerve, resulting in progressive sensorineural hearing loss, tinnitus, and impaired balance (1). Approximately 95% of adults with NF2 develop vestibular schwannomas at a mean age of 26 years (26,68). The presence of bilateral vestibular schwannomas is highly suggestive of NF2.

Schwannomas may also involve other cranial nerves, spinal nerve roots, and peripheral nerves. At pathologic analysis, schwannomas are encapsulated masses of pure Schwann cells around the nerve that contain areas of intertwining fascicles (Antoni A pattern) and loose cellular arrangements (Antoni B pattern) (69).

At CT, schwannomas manifest as hypoattenuating to isoattenuating masses, relative to the spinal cord, and are often associated with calcifications (70). However, calcifications are not seen with vestibular schwannomas (71). Larger vestibular schwannomas may widen the internal auditory canal, portending poor postoperative hearing function due to involvement of the cochlear nerve (71). At MRI, schwannomas are iso- or hypointense on T1-weighted images and hyperintense on T2-weighted images (relative to the brain), typically in a gyriform pattern that reflects their leptomen-

ingeal pattern of spread (70). They demonstrate heterogeneous enhancement due to necrosis, hemorrhage, or cystic changes (Fig 24).

Large vestibular schwannomas may manifest with concerning findings, such as brainstem or cerebellar compression, tonsillar herniation, hydrocephalus, or peritumor edema (71). In the spine, they are intradural extramedullary masses (Fig 25), commonly found at the level of C1 (4).

Progressive tumor growth leading to brainstem compression and hearing loss warrants surgical removal and possible auditory brainstem or cochlear implant. Stereotactic radiosurgery can be considered for smaller tumors, poor surgical candidates, and large tumors after subtotal resection (Fig 26) (1,71). Surgical resection is also performed for spinal schwannomas causing compressive symptoms (1,71). Targeted therapies, such as bevacizumab (monoclonal antibody) and brigatinib (kinase inhibitor), are being explored (3).

Meningiomas.—Intracranial and spinal meningiomas are the second most common tumors in NF2 (69). They are dural-based tumors with evidence of meningotheial cell differentiation and have a wide range of histologic appearances; the fibrous histologic subtype is most common in NF2 (70). The presence of multiple meningiomas is a key feature in NF2, which manifests in 50% of cases (70).

They are often located supratentorially along the falx cerebri and around the frontal, temporal, and parietal regions but may occur anywhere in the CNS. Patients are often asymptomatic, although headaches can occur when meningiomas become large (4). If meningiomas are located in the optic nerve sheath, skull base, or spinal canal, other compressive symptoms may manifest (65).

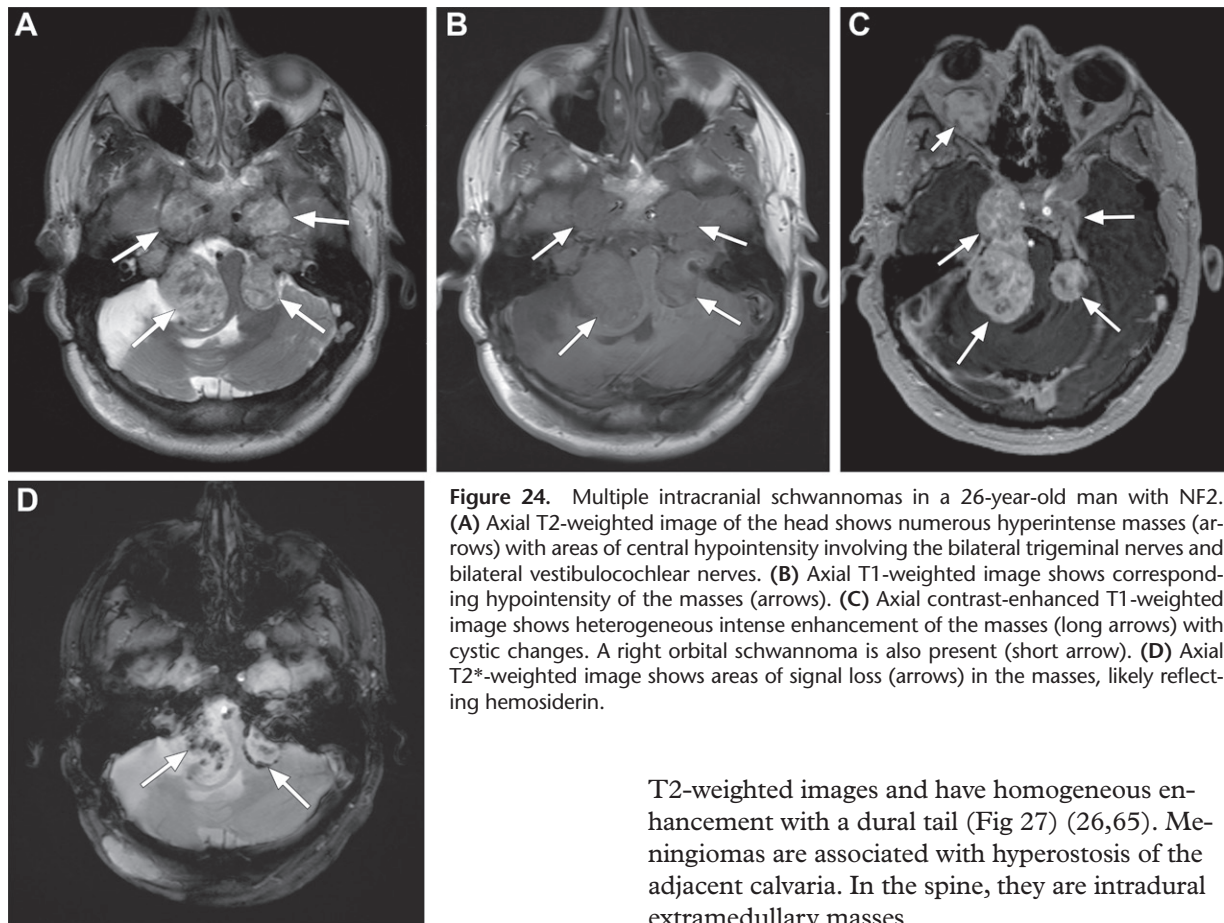


Figure 24. Multiple intracranial schwannomas in a 26-year-old man with NF2. (A) Axial T2-weighted image of the head shows numerous hyperintense masses (arrows) with areas of central hypointensity involving the bilateral trigeminal nerves and bilateral vestibulocochlear nerves. (B) Axial T1-weighted image shows corresponding hypointensity of the masses (arrows). (C) Axial contrast-enhanced T1-weighted image shows heterogeneous intense enhancement of the masses (long arrows) with cystic changes. A right orbital schwannoma is also present (short arrow). (D) Axial T2*-weighted image shows areas of signal loss (arrows) in the masses, likely reflecting hemosiderin.

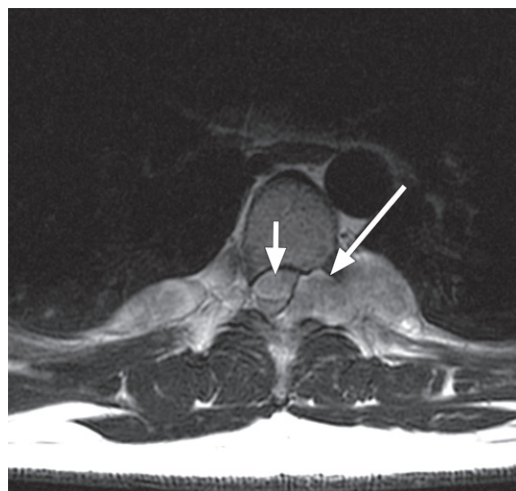


Figure 25. Multiple spinal schwannomas with spinal cord compression in a 25-year-old man with NF2. Axial contrast-enhanced T1-weighted image at the level of T6 shows a heterogeneously enhancing ventral intradural extramedullary mass (short arrow) that compresses the spinal cord. An additional enhancing mass (long arrow) along the left neural foramen extends into the spinal canal and contributes to the spinal cord compression.

At CT, meningiomas are dural-based hyperattenuating masses with avid enhancement. At MRI, they are isointense to gray matter on both T1- and

T2-weighted images and have homogeneous enhancement with a dural tail (Fig 27) (26,65). Meningiomas are associated with hyperostosis of the adjacent calvaria. In the spine, they are intradural extramedullary masses.

Complete resection is performed safely for most symptomatic meningiomas, although it may be limited for meningiomas arising from the optic nerve sheath or skull base (4,65). Adjuvant stereotactic radiosurgery may be considered in these cases.

Ependymomas.—Ependymomas are low-grade intramedullary tumors, occurring in up to 53% of individuals with NF2 (70). They often occur in the cervical spinal cord or at the cervicomedullary junction (86%), although they can rarely occur intracranially (72). Multiple spinal cord ependymomas are characteristically seen in NF2. Patients are often asymptomatic owing to the indolent nature of these tumors but can develop back pain and neurologic changes with tumor growth (1,65). At histopathologic analysis, ependymomas generally demonstrate well-delineated moderate cellularity with round-oval nuclei and occasional perivascular pseudorosettes and ependymal rosettes, although other histologic subtypes can be seen (65,70).

At MRI, the intramedullary masses are isointense or slightly hyperintense on T1-weighted images and hyperintense on T2-weighted images (relative to the cord), with homogeneous enhancement. When there are multiple lesions, they resemble a string of pearls on contrast-enhanced images (Fig 28). A hemosiderin cap may be seen

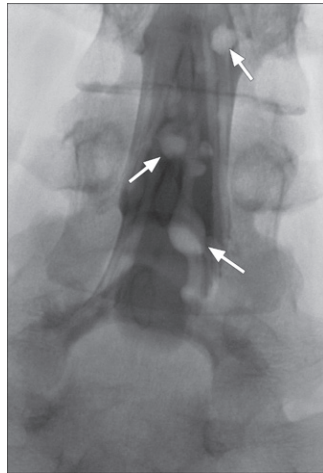


Figure 26. Multiple spinal schwannomas in a 15-year-old girl with NF2 and recurrent schwannomas involving the C5–T1 levels. Fluoroscopy-guided myelogram of the lower lumbar spine shows multiple round well-defined masses (arrows) along the spinal nerve roots before she was placed in the Trendelenburg position in an attempt to evaluate the lower cervical spine. Hardware at the level of the lower cervical spine limited evaluation with MRI. The study was performed for radiation treatment planning.

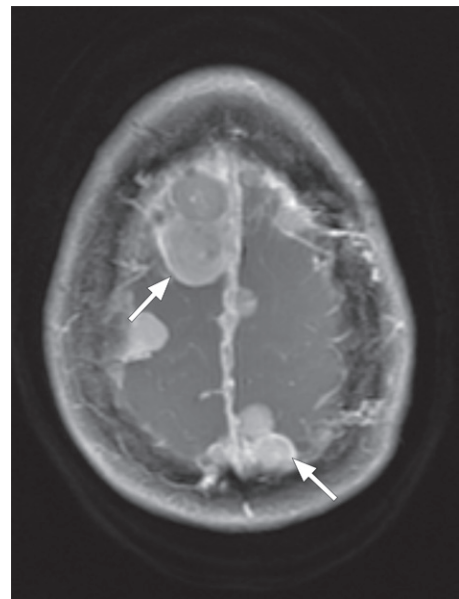


Figure 27. Multiple meningiomas in a 37-year-old woman with NF2. Axial contrast-enhanced T1-weighted image of the brain shows multiple homogeneously enhancing dural-based masses (arrows), many of which are along the falx cerebri.

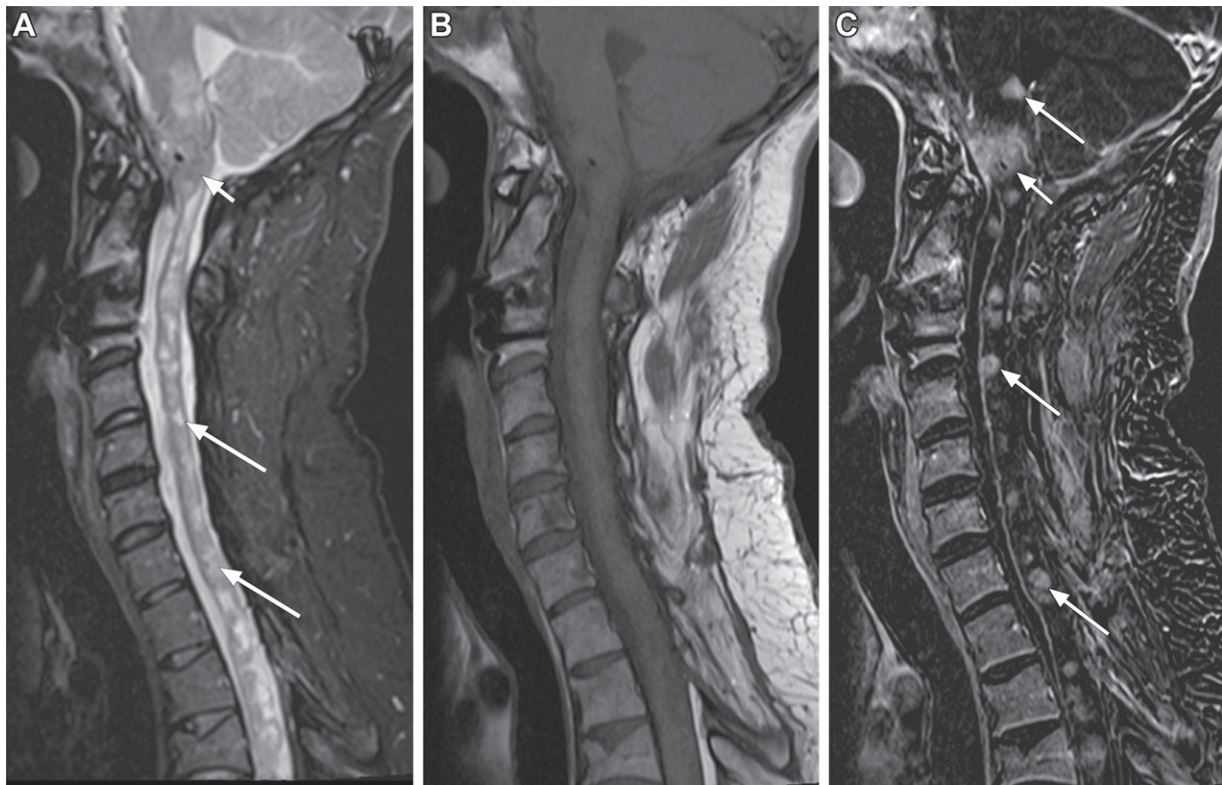


Figure 28. Spinal cord ependymomas and retroclival meningioma in a 32-year-old man with NF2. **(A)** Sagittal T2-weighted image of the cervical spine shows numerous intramedullary hyperintense lesions (long arrows) throughout the cervicomedullary junction and cervical spinal cord. A lesion in the medulla is also seen. There is an isointense retroclival mass (short arrow), which compresses the cervicomedullary junction. **(B)** Sagittal T1-weighted image shows corresponding isointensity or slight hyperintensity of the masses. **(C)** Sagittal contrast-enhanced subtraction T1-weighted image shows homogeneous enhancement of the intramedullary masses (long arrows), which resemble a string of pearls, consistent with ependymomas. The retroclival mass (short arrow) also enhances and represents a meningioma.

Table 5: Management Recommendations for Common NF1-related Manifestations

Manifestation	Management
Dermal and subcutaneous neurofibromas	Surgical removal, laser ablation, electrodesiccation
Plexiform neurofibromas	Surgical removal, mTOR and MEK inhibitors
Malignant PNSTs	Surgical removal; radiation therapy or chemotherapy for extensive or residual disease
Optic pathway glioma	Chemotherapy if symptomatic; RAS and mTOR blockers; surgery for severe symptoms Radiation therapy generally not appropriate owing to risk for development of secondary malignancy
Non-optic pathway glioma	Shunt for hydrocephalus; surgical resection, radiation therapy, or chemotherapy if symptomatic or progressive
Gastrointestinal stromal tumor (GIST)	Surgical removal
Pheochromocytoma or paraganglioma	Surgical resection; chemotherapy if growing or unresectable; adjuvant radiation therapy if large
Neuroendocrine neoplasms, peri-ampullary duodenum or near the ampulla of Vater	Pancreaticoduodenectomy if large (>2 cm); endoscopic resection if small (<2 cm)
Scoliosis	Spinal fusion if dystrophic; bracing if nondystrophic
Bone dysplasia with fractures	Bracing for fracture prevention; bone grafting, intramedullary rod placement, or external fixation for fractures
Low bone mineral density	Vitamin D supplementation
Renal artery stenosis	Renal artery reimplantation, bypass, renal arterioplasty, resection of stenosis with reanastomosis
Moyamoya disease	Revascularization

Sources.—References 1, 3, 15, 20, and 44.

Note.—MEK = mitogen-activated protein kinase kinase, mTOR = mammalian target of rapamycin.

Table 6: Management Recommendations for Common NF2-related Manifestations

Manifestation	Management
Schwannomas	Surgical resection with or without auditory brainstem implant if symptomatic with brainstem compression; stereotactic radiosurgery for smaller tumors, after subtotal resection, or for poor surgical candidates; bevacizumab for size reduction
Meningiomas	Surgical resection if symptomatic; adjuvant stereotactic radiosurgery for residual or surgically inaccessible disease
Ependymomas	Surgical resection if symptomatic

Sources.—References 1, 3, and 65.

at the superior and inferior poles of the tumor (65). Since ependymomas are often asymptomatic, they usually undergo surveillance (4). In symptomatic cases, surgical resection is usually curative (65).

Management and Surveillance

Although many patients with NF1 survive into adulthood, average life expectancy is decreased to 54 years, largely due to malignancy (5). The average survival in NF2 is slightly higher at 62 years (4). Thus, a multidisciplinary approach is essential for lifelong management and surveillance of NF1 and NF2. Management recommendations for common manifestations are summarized in Tables 5 and 6.

NF1 surveillance includes annual evaluation for cutaneous, ophthalmic, and neurologic manifestations and blood pressure measurement (17). Surveillance for asymptomatic patients includes screening mammography starting at the age of 30 years and dual-energy x-ray absorptiometry (DEXA) for osteoporosis (11,17). Suggestive symptoms should prompt targeted imaging, such as that for evaluating CNS gliomas, plexiform neurofibromas, and malignant PNSTs (17).

Recently, whole-body MRI has emerged as a potential option for NF1 surveillance, owing to its lack of radiation and new more efficient imaging protocols. Although whole-body MRI can allow early detection of many NF1 manifestations, it

Table 7: NF1 Surveillance Recommendations

Organ System	Surveillance Recommendations
Cutaneous	Annual dermatologic examination
Breast	Annual screening mammography starting at age 30 years
Ophthalmic	Ophthalmic examination every month from birth to 8 years, then annually until 16 years, then every 2 years afterward
CNS	Annual review of growth and sexual development for hypothalamic dysfunction Annual neurologic examination Annual examination for learning disabilities, attention deficit hyperactivity disorder, and social perception problems MRI of the brain and spine with and without contrast material for patients with unexplained or progressive symptoms
Musculoskeletal	Annual examination for scoliosis and pseudarthrosis
Vascular	Annual blood pressure measurements

Sources.—References 15 and 17.

Table 8: NF2 Surveillance Recommendations

Organ System	Surveillance Recommendations
Cutaneous	Dermatologic examination at baseline and at 18–20 years
Ophthalmic	Ophthalmic examination at baseline and at 18–20 years
CNS	Audiologic examination at baseline and at 18–20 years Annual MRI of the brain with and without contrast material including internal auditory canals; every 3–6 months if at high risk for brainstem compression or compromise of facial or vestibular nerves MRI of the spine with and without contrast material every 3 years if there are spinal tumors MRI of the spine with and without contrast material every 5 years if there are no spinal tumors

Sources.—References 4 and 17.

may be particularly useful in detecting and quantifying PNSTs (17) (Fig E9). This is important, as both an increased number and whole-body volume of PNSTs have been associated with an increased risk of malignant PNST development (73). Additionally, PNSTs are often asymptomatic and can cross anatomic boundaries, supporting use of whole-body MRI over localized imaging. However, owing to limited data, a consensus has not yet been reached on routine use of whole-body MRI in asymptomatic patients with NF1 (17).

PET/MRI is also a recently explored modality, adding the functional information of ^{18}F -fluorodeoxyglucose (FDG) PET to the benefits of whole-body MRI. As with PET/CT, it may be useful in identifying malignant PNSTs, with a recent study of ^{18}F -FDG PET/MRI finding higher uptake in malignant PNSTs than in benign plexiform neurofibromas (74) (Fig E10). PET/MRI has been shown to reduce radiation exposure by almost 50% over PET/CT and may be more useful in closely approximated lesions (75).

NF2 surveillance includes cutaneous, ophthalmic, audiologic, and neurologic evaluations with baseline brain MRI, including thin sections through the internal auditory canal. Regardless of symptoms, surveillance MRI is performed for intracranial and spinal tumors. Whole-body MRI may also have a role in NF2, although its use is less clear, since NF2-related PNSTs tend to be benign. However, early detection of PNSTs may be helpful to guide management (17). Surveillance recommendations are summarized in Tables 7 and 8.

Conclusion

Although NF1 and NF2 share a common name, they are clinically distinct autosomal dominant inherited neurocutaneous conditions caused by mutations in the *NF1* and *NF2* genes, respectively, resulting in development of various benign and malignant tumors that are associated with substantial morbidity and mortality. Key manifestations of NF1 include café-au-lait macules,

freckling, neurofibromas, optic pathway gliomas, Lisch nodules, and various osseous lesions. NF2 classically manifests with vestibular schwannomas, multiple meningiomas, and spinal cord ependymomas. Radiologists play a vital role in diagnosis and lifelong surveillance of patients with these conditions.

Acknowledgments.—We thank Christine Cooky Menias, MD, for her mentorship and guidance. We thank Kelly Kage, MFA, for the illustration in Figure 1.

Disclosures of conflicts of interest.—K.M.E. Editorial board member of *RadioGraphics*.

References

- Ferner RE. The neurofibromatoses. *Pract Neurol* 2010;10(2):82–93.
- Jouhilahti EM, Peltonen S, Heape AM, Peltonen J. The pathoetiology of neurofibromatosis 1. *Am J Pathol* 2011;178(5):1932–1939.
- Amaravathi A, Oblinger JL, Welling DB, Kinghorn AD, Chang LS. Neurofibromatosis: Molecular Pathogenesis and Natural Compounds as Potential Treatments. *Front Oncol* 2021;11:698192.
- Lloyd SKW, Evans DGR. Neurofibromatosis type 2 (NF2): diagnosis and management. *Handb Clin Neurol* 2013;115:957–967.
- Kresak JL, Walsh M. Neurofibromatosis: A Review of NF1, NF2, and Schwannomatosis. *J Pediatr Genet* 2016;5(2):98–104.
- Kluger N, Perrochia H, Guillot B. Pelvic mass in von Recklinghausen's neurofibromatosis: diagnostic issues—a case report. *Cases J* 2009;2:191.
- Legius E, Messiaen L, Wolkenstein P, et al. Revised diagnostic criteria for neurofibromatosis type 1 and Legius syndrome: an international consensus recommendation. *Genet Med* 2021;23(8):1506–1513.
- Smith MJ, Bowers NL, Bulman M, et al. Revisiting neurofibromatosis type 2 diagnostic criteria to exclude LZTR1-related schwannomatosis. *Neurology* 2017;88(1):87–92. [Published correction appears in *Neurology* 2017;89(2):215.]
- Ozarlan B, Russo T, Argenziano G, Santoro C, Piccolo V. Cutaneous Findings in Neurofibromatosis Type 1. *Cancers (Basel)* 2021;13(3):463.
- Nunley KS, Gao F, Albers AC, Bayliss SJ, Gutmann DH. Predictive value of café au lait macules at initial consultation in the diagnosis of neurofibromatosis type 1. *Arch Dermatol* 2009;145(8):883–887.
- Ferner RE, Huson SM, Thomas N, et al. Guidelines for the diagnosis and management of individuals with neurofibromatosis 1. *J Med Genet* 2007;44(2):81–88.
- Zulfiqar M, Lin M, Ratkowski K, Gagnon MH, Menias C, Siegel CL. Imaging Features of Neurofibromatosis Type 1 in the Abdomen and Pelvis. *AJR Am J Roentgenol* 2021;216(1):241–251.
- Fortman BJ, Kuszyk BS, Urban BA, Fishman EK. Neurofibromatosis type 1: a diagnostic mimicker at CT. *RadioGraphics* 2001;21(3):601–612.
- Patel NB, Stacy GS. Musculoskeletal manifestations of neurofibromatosis type 1. *AJR Am J Roentgenol* 2012;199(1):W99–W106.
- Gutmann DH, Ferner RE, Listernick RH, Korf BR, Wolters PL, Johnson KJ. Neurofibromatosis type 1. *Nat Rev Dis Primers* 2017;3:17004.
- Mautner VF, Asuagbor FA, Dombi E, et al. Assessment of benign tumor burden by whole-body MRI in patients with neurofibromatosis 1. *Neuro Oncol* 2008;10(4):593–598.
- Ahlawat S, Blakeley JO, Langmead S, Belzberg AJ, Fayad LM. Current status and recommendations for imaging in neurofibromatosis type 1, neurofibromatosis type 2, and schwannomatosis. *Skeletal Radiol* 2020;49(2):199–219.
- Da Silva AV, Rodrigues FR, Pureza M, Lopes VGS, Cunha KS. Breast cancer and neurofibromatosis type 1: a diagnostic challenge in patients with a high number of neurofibromas. *BMC Cancer* 2015;15:183.
- Kinori M, Hodgson N, Zeid JL. Ophthalmic manifestations in neurofibromatosis type 1. *Surv Ophthalmol* 2018;63(4):518–533.
- Ferner RE, Gutmann DH. Neurofibromatosis type 1 (NF1): diagnosis and management. *Handb Clin Neurol* 2013;115:939–955.
- Friedman JM, Birch PH. Type 1 neurofibromatosis: a descriptive analysis of the disorder in 1,728 patients. *Am J Med Genet* 1997;70(2):138–143.
- Russo C, Russo C, Cascone D, et al. Non-Oncological Neuroradiological Manifestations in NF1 and Their Clinical Implications. *Cancers (Basel)* 2021;13(8):1831.
- Sánchez Marco SB, López Pisón J, Calvo Escribano C, González Viejo I, Miramar Gallart MD, Samper Villagrasa P. Neurological manifestations of neurofibromatosis type 1: our experience. *Neurologia (Engl Ed)* 2019. 10.1016/j.nrl.2019.05.003. Published online July 17, 2019.
- Duong TA, Sbidian E, Valeyrie-Allanore L, et al. Mortality associated with neurofibromatosis 1: a cohort study of 1895 patients in 1980–2006 in France. *Orphanet J Rare Dis* 2011;6:18.
- Gill DS, Hyman SL, Steinberg A, North KN. Age-related findings on MRI in neurofibromatosis type 1. *Pediatr Radiol* 2006;36(10):1048–1056.
- Rodriguez D, Young Poussaint T. Neuroimaging findings in neurofibromatosis type 1 and 2. *Neuroimaging Clin N Am* 2004;14(2):149–170. vii.
- Feldmann R, Schuierer G, Wessel A, Neveling N, Weglage J. Development of MRI T2 hyperintensities and cognitive functioning in patients with neurofibromatosis type 1. *Acta Paediatr* 2010;99(11):1657–1660.
- Hyman SL, Gill DS, Shores EA, Steinberg A, North KN. T2 hyperintensities in children with neurofibromatosis type 1 and their relationship to cognitive functioning. *J Neurol Neurosurg Psychiatry* 2007;78(10):1088–1091.
- Piscitelli O, Digilio MC, Capolino R, Longo D, Di Ciommo V. Neurofibromatosis type 1 and cerebellar T2-hyperintensities: the relationship to cognitive functioning. *Dev Med Child Neurol* 2012;54(1):49–51.
- Baudou E, Nemmi F, Biotteau M, Maziero S, Peran P, Chaix Y. Can the Cognitive Phenotype in Neurofibromatosis Type 1 (NF1) Be Explained by Neuroimaging? A Review. *Front Neurol* 2020;10:1373.
- Kandt RS. Tuberous sclerosis complex and neurofibromatosis type 1: the two most common neurocutaneous diseases. *Neurol Clin* 2003;21(4):983–1004.
- Listernick R, Ferner RE, Liu GT, Gutmann DH. Optic pathway gliomas in neurofibromatosis-1: controversies and recommendations. *Ann Neurol* 2007;61(3):189–198.
- Listernick R, Charrow J, Greenwald M, Mets M. Natural history of optic pathway tumors in children with neurofibromatosis type 1: a longitudinal study. *J Pediatr* 1994;125(1):63–66.
- Fried I, Tabori U, Tihan T, Reginald A, Bouffet E. Optic pathway gliomas: a review. *CNS Oncol* 2013;2(2):143–159.
- Sellmer L, Farschtschi S, Marangoni M, et al. Non-optic glioma in adults and children with neurofibromatosis 1. *Orphanet J Rare Dis* 2017;12(1):34.
- Pollack IF, Shultz B, Mulvihill JJ. The management of brainstem gliomas in patients with neurofibromatosis 1. *Neurology* 1996;46(6):1652–1660.
- Dunn IF, Agarwalla PK, Papanastassiou AM, Butler WE, Smith ER. Multiple pilocytic astrocytomas of the cerebellum in a 17-year-old patient with neurofibromatosis type I. *Childs Nerv Syst* 2007;23(10):1191–1194.
- Lobbous M, Bernstock JD, Coffee E, et al. An Update on Neurofibromatosis Type 1-Associated Gliomas. *Cancers (Basel)* 2020;12:114.
- Gajeski BL, Kettner NW, Awwad EE, Boesch RJ. Neurofibromatosis type I: clinical and imaging features of Von Recklinghausen's disease. *J Manipulative Physiol Ther* 2003;26(2):116–127.
- Derdabi I, Jouadi HE, Edderaï M. Dural ectasia: a manifestation of type 1 neurofibromatosis. *Pan Afr Med J* 2018;31:226.

41. Yu YH, Wu JT, Ye J, Chen MX. Radiological findings of malignant peripheral nerve sheath tumor: reports of six cases and review of literature. *World J Surg Oncol* 2016;14:142.
42. Wasa J, Nishida Y, Tsukushi S, et al. MRI features in the differentiation of malignant peripheral nerve sheath tumors and neurofibromas. *AJR Am J Roentgenol* 2010;194(6):1568–1574.
43. Ferner RE, Golding JF, Smith M, et al. [18F]2-fluoro-2-deoxy-D-glucose positron emission tomography (FDG PET) as a diagnostic tool for neurofibromatosis 1 (NF1) associated malignant peripheral nerve sheath tumours (MPNSTs): a long-term clinical study. *Ann Oncol* 2008;19(2):390–394.
44. Dare AJ, Gupta AA, Thippavong S, Miettinen M, Gladly RA. Abdominal neoplastic manifestations of neurofibromatosis type 1. *Neurooncol Adv* 2020;2(suppl 1):i124–i133.
45. Prudner BC, Ball T, Rathore R, Hirbe AC. Diagnosis and management of malignant peripheral nerve sheath tumors: current practice and future perspectives. *Neurooncol Adv* 2019;2(suppl 1):i40–i49.
46. Oikonomou A, Vadikolias K, Birbilis T, Bouros D, Prassopoulos P. HRCT findings in the lungs of non-smokers with neurofibromatosis. *Eur J Radiol* 2011;80(3):e520–e523.
47. Alves Júnior SF, Zanetti G, Alves de Melo AS, et al. Neurofibromatosis type 1: state-of-the-art review with emphasis on pulmonary involvement. *Respir Med* 2019;149:9–15.
48. Barahona-Garrido J, Aguirre-Gutiérrez R, Gutiérrez-Manjarrez JJ, et al. Association of GIST and somatostatinoma in a patient with type-1 neurofibromatosis: is there a common pathway? *Am J Gastroenterol* 2009;104(3):797–799.
49. Salvi PF, Lorenzon L, Caterino S, Antonino L, Antonelli MS, Balducci G. Gastrointestinal stromal tumors associated with neurofibromatosis 1: a single centre experience and systematic review of the literature including 252 cases. *Int J Surg Oncol* 2013;2013:398570.
50. Walther MM, Herring J, Enquist E, Keiser HR, Linehan WM. von Recklinghausen's disease and pheochromocytomas. *J Urol* 1999;162(5):1582–1586.
51. Nishi T, Kawabata Y, Hari Y, et al. A case of pancreatic neuroendocrine tumor in a patient with neurofibromatosis-1. *World J Surg Oncol* 2012;10:153.
52. Ferrari A, Bisogno G, Macaluso A, et al. Soft-tissue sarcomas in children and adolescents with neurofibromatosis type 1. *Cancer* 2007;109(7):1406–1412.
53. Stay EJ, Vawter G. The relationship between nephroblastoma and neurofibromatosis (Von Recklinghausen's disease). *Cancer* 1977;39(6):2550–2555.
54. Yucel C, Budak S, Kisa E, Celik O, Kozacioglu Z. The Rare Togetherness of Bladder Leiomyoma and Neurofibromatosis. *Case Rep Urol* 2018;2018:2302918.
55. Aleksandrovych V, Bereza T, Sajewicz M, Walocha JA, Gil K. Uterine fibroid: common features of widespread tumor (review article). *Folia Med Cracov* 2015;55(1):61–75.
56. Murase E, Siegelman ES, Outwater EK, Perez-Jaffe LA, Tureck RW. Uterine leiomyomas: histopathologic features, MR imaging findings, differential diagnosis, and treatment. *RadioGraphics* 1999;19(5):1179–1197.
57. Li HM, Liu J, Qiang JW, Zhang H, Zhang GF, Ma F. Diffusion-Weighted Imaging for Differentiating Uterine Leiomyosarcoma From Degenerated Leiomyoma. *J Comput Assist Tomogr* 2017;41(4):599–606.
58. Duc NM, Keserci B. Review of influential clinical factors in reducing the risk of unsuccessful MRI-guided HIFU treatment outcome of uterine fibroids. *Diagn Interv Radiol* 2018;24(5):283–291.
59. Landry JP, Schertz KL, Chiang YJ, et al. Comparison of Cancer Prevalence in Patients With Neurofibromatosis Type 1 at an Academic Cancer Center vs in the General Population From 1985 to 2020. *JAMA Netw Open* 2021;4(3):e210945.
60. Afsar CU, Kara IO, Kozat BK, Demiryürek H, Duman BB, Doran F. Neurofibromatosis type 1, gastrointestinal stromal tumor, leiomyosarcoma and osteosarcoma: four cases of rare tumors and a review of the literature. *Crit Rev Oncol Hematol* 2013;86(2):191–199.
61. Marko J, Wolfman DJ. From the Radiologic Pathology Archives: Retroperitoneal Leiomyosarcoma. *RadioGraphics* 2018;38(5):1403–1420.
62. Crawford AH, Schorry EK. Neurofibromatosis update. *J Pediatr Orthop* 2006;26(3):413–423.
63. Casselman ES, Mandell GA. Vertebral scalloping in neurofibromatosis. *Radiology* 1979;131(1):89–94.
64. Solanki C, Ramachandran S, Devi BI, Sharma R. Calvarial defects in the region of the lambdoid suture in neurofibromatosis type-1 patients. *J Pediatr Neurosci* 2015;10(1):22–24.
65. Asthagiri AR, Parry DM, Butman JA, et al. Neurofibromatosis type 2. *Lancet* 2009;373(9679):1974–1986.
66. Evans DG. Neurofibromatosis type 2 (NF2): a clinical and molecular review. *Orphanet J Rare Dis* 2009;4:16.
67. Bosch MM, Boltshauser E, Harpes P, Landau K. Ophthalmologic findings and long-term course in patients with neurofibromatosis type 2. *Am J Ophthalmol* 2006;141(6):1068–1077.
68. Parry DM, Eldridge R, Kaiser-Kupfer MI, Bouzas EA, Pikus A, Patronas N. Neurofibromatosis 2 (NF2): clinical characteristics of 63 affected individuals and clinical evidence for heterogeneity. *Am J Med Genet* 1994;52(4):450–461.
69. Evans DGR, Baser ME, O'Reilly B, et al. Management of the patient and family with neurofibromatosis 2: a consensus conference statement. *Br J Neurosurg* 2005;19(1):5–12.
70. Coy S, Rashid R, Stemmer-Rachamimov A, Santagata S. An update on the CNS manifestations of neurofibromatosis type 2. *Acta Neuropathol (Berl)* 2020;139(4):643–665. [Published correction appears in *Acta Neuropathol* 2020;139(4):667.]
71. Lin EP, Crane BT. The Management and Imaging of Vestibular Schwannomas. *AJNR Am J Neuroradiol* 2017;38(11):2034–2043.
72. Kresbach C, Dorostkar MM, Suwala AK, et al. Neurofibromatosis type 2 predisposes to ependymomas of various localization, histology, and molecular subtype. *Acta Neuropathol (Berl)* 2021;141(6):971–974.
73. Nguyen R, Jett K, Harris GJ, Cai W, Friedman JM, Mautner VF. Benign whole body tumor volume is a risk factor for malignant peripheral nerve sheath tumors in neurofibromatosis type 1. *J Neurooncol* 2014;116(2):307–313.
74. Reinert CP, Schuhmann MU, Bender B, et al. Comprehensive anatomical and functional imaging in patients with type I neurofibromatosis using simultaneous FDG-PET/MRI. *Eur J Nucl Med Mol Imaging* 2019;46(3):776–787.
75. Raad RA, Lala S, Allen JC, et al. Comparison of hybrid 18F-fluorodeoxyglucose positron emission tomography/magnetic resonance imaging and positron emission tomography/computed tomography for evaluation of peripheral nerve sheath tumors in patients with neurofibromatosis type 1. *World J Nucl Med* 2018;17(4):241–248.